

TUTDoR

Response of cyclopia subternata to drought stress assessment of leaf composition, proteomics and product quality.

Item Type	Article
Authors	Mabizela, G.S.;Van der Rijst, M.;Slabbert, M.M.;Mathabe, P.;Muller, M.;DeBeer, D.;Stander, M.;Colling, J.;Walczak, B.;Joubert, E.;Bester, C.
DOI	http://dx.doi.org/10.3390/rs12101661
Publisher	Elsevier B.V.
Rights	Attribution-NonCommercial-ShareAlike 4.0 International
Download date	2026-05-09 17:22:22
Item License	http://creativecommons.org/licenses/by-nc-sa/4.0/
Link to Item	https://hdl.handle.net/20.500.14519/1204



Response of *Cyclopia subternata* to drought stress – assessment of leaf composition, proteomics and product quality



G.S. Mabizela^{a,b,1,*}, M. van der Rijst^c, M.M. Slabbert^b, P. Mathabe^{d,2}, M. Muller^e, D. de Beer^{e,f}, M. Stander^g, J. Colling^g, B. Walczak^h, E. Joubert^{e,f}, C. Bester^a

^a Crop Development Division, Agricultural Research Council (ARC), Infruitec-Nietvoorbij, Private Bag X5026, Stellenbosch 7599, South Africa

^b Department of Horticulture, Tshwane University of Technology, Private Bag X680, Pretoria 0001, South Africa

^c Biometry Unit, ARC, Private Bag X5026, Stellenbosch 7599, South Africa

^d Post-Harvest and Agro-Processing Technologies, ARC Infruitec-Nietvoorbij, Private Bag X5026, Stellenbosch 7599, South Africa

^e Department of Food Science, Stellenbosch University, Private Bag X1, Matieland Stellenbosch 7602, South Africa

^f Plant Bioactives Group, Post-Harvest and Agro-Processing Technologies, ARC Infruitec-Nietvoorbij, Private Bag X5026, Stellenbosch 7599, South Africa

^g Central Analytical Facility, Stellenbosch University, Private Bag X1, Matieland Stellenbosch 7602, South Africa

^h Institute of Chemistry, University of Silesia, Katowice, Poland

ARTICLE INFO

Article History:

Received 28 November 2022

Revised 21 June 2023

Accepted 19 July 2023

Available online xxx

Edited by Dr N. Masondo

Keywords:

Carbohydrates

Cyclopia subternata

Drought response

Herbal tea

Polyphenols

Proline

Two-dimensional polyacrylamide gel

electrophoresis

Relative water content

Sensory profile

ABSTRACT

Honeybush tea is made from the fynbos plant *Cyclopia subternata*, which is unique to South Africa. Cultivation takes place in its natural environment, which has a Mediterranean climate with dry summers and wet winters. During the summer, the plant is vulnerable to drought, an abiotic stress factor that is likely to affect its development and yield. This study investigated the effect of drought stress for a short duration on the leaf, as well as the quality of the herbal tea. Protein expression in the leaf was measured to gain insight into possible mechanisms used by the plant to cope with drought stress conditions. Fifteen-month-old *C. subternata* plants were subjected to three water treatments (control, moderately-stressed (MS), and severely-stressed (SS)) for ten days. Leaves were sampled at regular intervals throughout the treatment period to determine their relative water content (RWC). Leaves were also sampled on the 11th day for untargeted and targeted chemical composition and protein expression analyses. The remaining leaves and stems were processed to obtain the herbal tea. Descriptive sensory analysis of the herbal tea was performed to determine whether drought stress affected product quality. RWC was substantially higher ($p < 0.05$) in the control plants (100%) than in the MS and SS treated plants (83–90% and 47%, respectively). Untargeted analysis revealed that drought stress considerably altered leaf chemical composition. According to targeted analysis, the proline content of SS treated plants increased more than 40-fold when compared to the control, however, the treatments had no effect on the total carbohydrate and major phenolic compound content of the leaves, nor on the sensory quality of the herbal tea. Differences in the expression of 27 proteins, 24 of which were identified using proteomic analysis, were observed. During drought stress, 17 of these proteins increased, whereas seven decreased. Thirteen of the 24 identified proteins produced statistically significant results based on their Byonic scores. The findings laid the foundation for future research into the functions of drought response genes in *Cyclopia* species, as well as helping with the identification of stress-tolerant honeybush genotypes.

© 2023 The Author(s). Published by Elsevier B.V. on behalf of SAAB. This is an open access article under the CC BY license (<http://creativecommons.org/licenses/by/4.0/>)

* Corresponding author at: Crop Development Division, ARC Infruitec-Nietvoorbij, Private Bag X5026, Stellenbosch 7599, South Africa.

E-mail address: gugu.mabizela@westerncape.gov.za (G.S. Mabizela).

¹ Present address: RTDS: Plant Sciences, Department of Agriculture: Western Cape, Private Bag X1, Elsenburg, 7607, South Africa

² Royal Agriculture University, School of Agriculture Food and Environment, Stroud Road, GL76JS, Cirencester, UK

1. Introduction

Cyclopia subternata, a fynbos plant with trifoliate, flattened, oblong leaves (Slabbert et al., 2011), is one of the *Cyclopia* species (Fabaceae family) domesticated for honeybush tea production. Its cultivation takes place in the southwestern part of South Africa, an area with a Mediterranean climate, characterised by long, dry summers and wet, cold winters. Drought is thus already a problem throughout the summer months, and rising temperatures caused by

global warming are likely to exacerbate drought conditions due to increased evapotranspiration (Wu et al., 2022). Rainfall in the Western Cape Province is anticipated to be 30% lower by 2050 than at present (Grosling, 2019).

In comparison to other environmental stresses, drought is one environmental condition that significantly lowers crop productivity (Hura et al., 2022). Therefore, identifying and understanding all levels that regulate adaptive mechanisms and crop plant resilience in the context of drought stress is crucial when attempting to breed stress-tolerant cultivars. Despite this need, the response of the honeybush plant to drought stress is yet unknown, necessitating research that would assist in mitigating the risks associated with honeybush domestication and commercialisation. Plants have evolved various protective mechanisms such as drought escape, drought avoidance and drought tolerance (Gonzalez, 2023) over time that allow them to acclimatise to unfavourable environments for continued survival and growth (Hura et al., 2022). Since proteins are direct effectors of drought stress resistance (Zhou et al., 2023), the identification of key proteins connected to greater tolerance to adverse environmental factors is vital for the introduction of desired biological traits to a crop (Singh et al., 2022). Proteomics plays an essential role in the identification and categorisation of proteins according to their putative functions (Amnan et al., 2022). It has been applied in the field of crop abiotic stress-tolerance research to compare different proteomes (Kausar et al., 2022; Naik et al., 2023). Drought-responsive proteins, which showed significant changes in expression between normal and drought stress conditions, were identified in two wheat cultivars (Shayan et al., 2020). Proteomics of fennel showed that photosynthesis was decreased in a drought-sensitive genotype but increased in a drought-tolerant genotype (Khodadadi et al., 2017).

Proteomics investigations on honeybush have not been reported before, making this the first study to investigate the response of honeybush plants subjected to drought stress for a short duration and its effect on the proteomics, leaf chemical composition and herbal tea quality. Investigating proteome changes in honeybush caused by drought stress would increase understanding of the molecular mechanism of drought resistance in honeybush at the protein level. When subjected to drought stress, plants first undergo morphological and biochemical changes that lead to acclimation (Amnan et al., 2022; Luz et al., 2023), and as the drought worsens, it causes functional damage and abscission of plant parts (Goharrizi et al., 2021). When applied to *C. subternata*, this approach could lead to a better understanding of protein responses and functions of this legume.

The main aim of the present study was to determine how the proteome of *C. subternata* leaves alters in response to drought stress of relatively short duration. The relative water content of the leaves was determined to confirm drought stress while untargeted chemical analysis served to confirm that leaf composition was affected. Targeted analysis entailed quantification of the total carbohydrate, proline and phenolic content of the leaves. The sensory profile of the herbal tea product was determined to give a practical perspective on drought stress in terms of product quality.

2. Materials and methods

2.1. Experimental site and layout

A pot trial was conducted in the glasshouse facility at ARC Infruitec-Nietvoorbij, Stellenbosch, South Africa (33.9253° S, 18.8730° E). The experimental design was a completely randomised design and had one fixed factor, consisting of three treatments (levels), i.e. the control (well-watered, WW), moderately-stressed (MS) and severely-stressed (SS), with seven biological replicates per treatment. Each treatment × replicate combination consisted of eight *C. subternata* plants, with one shoot from each of the eight plants pooled to represent a replicate. The experiment had a total of 168 plants that

were randomly assigned to the different treatments. Fig. A1 (Supplementary information) gives the outline of the treatments and sample collection.

2.2. Drought stress treatment

Nine-month-old seedlings (a mixture of different *C. subternata* genotypes due to the shortage of plant material) were transplanted in early July 2018 into large pots (30 cm diameter, 28.5 cm height, with holes in the bottom) filled with a potting mixture of polystyrene balls: sandy soil: Canadian peat moss (3:3:3 v/v/v), a standard medium used for honeybush production. A fine Nylon net mesh (20 μm) was fitted at the bottom to allow air and water exchange but to prevent root passage. A layer of gravel stones was placed on top of the Nylon net to provide drainage. The plants were moved to the glasshouse where they were kept at an average temperature of 25 °C and watered as needed (using overhead sprinkler watering) for three months. A week before the drought treatment commenced, the plants were irrigated with tap water every third day to allow hardening off prior to subjecting them to a water deficit. Plants were randomly assigned between the three treatments, i.e. WW (control) (water maintained at 75% field capacity), MS (water maintained at 50% field capacity) and SS (water maintained at 30% field capacity). Tensiometers were randomly placed in pots throughout the experiment to monitor the soil moisture. The controls received 500 mL water every second day, the MS plants received 500 mL water every fourth day and SS plants received 500 mL water once on day zero whereafter watering was discontinued (Supplementary information, Fig. A1). The plants were stressed for a total of 10 days.

2.3. Measuring relative water content of leaves

The relative water content (RWC) of the leaves was determined according to a modified version of the method by Sade et al. (2015). Sampling of leaves for analysis took place during the treatment period in early November 2018, starting on day zero and thereafter every second day. Final sampling was done the day after the treatment period (day 11). The leaves were harvested midday between 12:00–12:30 pm. Briefly, the leaves were sampled by collecting the top (young) leaf of five branches/plant/treatment replicate. Each leaf was cut in half to facilitate water absorption to determine the turgid mass and placed immediately in a pre-weighed screw-cap glass vial (40 mL) to prevent moisture loss. The samples were transported to the laboratory in a cooler box without delay (within 10 min) where the vials were weighed (4 decimals) to determine the fresh mass (FM). Distilled water (2 mL) was then added to each vial to allow the cut leaves to rehydrate for 4 h in darkness. The rehydrated leaf samples were removed from the water, rapidly blotted with a paper towel to remove surface water and weighed to determine the turgid mass (TM). The samples were then dried to a constant mass (70 °C for 48 h) for determination of dry mass (DM).

The relative water content was calculated as:

$$\text{RWC}\% = (\text{FM} - \text{DM}) / (\text{TM} - \text{DM}) \times 100$$

2.4. Preparation of plant material

Following treatment, shoots were collected in batches from the different treatments. For determination of the total carbohydrate and phenolic content of the leaves, the top part (15 cm) of one shoot from each of the eight plants, representing a replicate of a treatment, was removed, pooled and dried intact under forced air circulation (3 m/s cross-flow) in a drying tunnel at 30 °C for 12 h. At completion of this drying stage, the leaves were only partially dried, but they could be easily separated from the stems without damage. Final drying took place in a vacuum oven at 40 °C for 16 h. The dried leaves were milled

to a fine powder, using a Retsch MM301 ball mill (Retsch GmbH, Haan, Germany). The milled samples were sealed in screw-cap glass vials and stored at 4 °C until analysis.

For determination of proline accumulation over the treatment period, the top part (15 mm) of five shoots of each plant per treatment replicate were removed, pooled, placed in re-sealable plastic bags (200 × 250 mm) and frozen in liquid nitrogen. The sampling took place every second day with the last sampling on day 10. Upon harvesting, the samples were placed immediately in an icebox and transported without delay to the laboratory where they were stored at –80 °C until further analysis.

The remaining plant material of a replicate was pooled and processed into 'fermented' (oxidised) honeybush tea according to a standard protocol (Mabizela et al., 2020). The 'tea-bag' fraction (<1.68 mm; >0.42 mm) was stored in sealed glass jars until sensory analysis.

2.5. Untargeted analysis of leaf composition

2.5.1. Near-infrared hyperspectral imaging (NIR-HSI) of leaf samples

The milled, dried leaf samples were transferred to circular plastic holders (40 mm diameter; 4 mm depth) and the surface was levelled before the hyperspectral images were acquired. The equipment consisted of a push-broom line scan HySpex SWIR-384 (short wave infrared) imaging system (Norsk Elektro Optikk A/S, Skedsmokorset, Norway) and Breeze® software (Version 2019.2.0, Prediktera AB, Umeå, Sweden) was used for data acquisition and initial analysis. The cameras were mounted on a laboratory rack with a translation stage and fitted with a 30 cm focal length lens that has a field of view of 9.5 cm. The imaging system comprised of an imaging spectrograph, coupled to a mercury cadmium telluride (MCT) sensor. The spectral range for the SWIR camera is from 950 – 2500 nm with a spectral resolution of 5.45 nm resulting in a total of 288 spectral bands. The spatial resolution when using the 30 cm lens is a pixel size of 0.247 mm and each line in the image consists of 384 pixels. Samples were illuminated by two 150 W halogen lamps (Ushio Lighting Inc., Japan), emitting light in the 400 – 2500 nm wavelength range. The lights were placed symmetrically 30 cm above the translation stage. The frame rate was set to 100 Hz and the integration time was set to 2103 μ s. Samples were imaged randomly and three technical replicates of each sample were analysed (the milled sample was mixed, flattened and analysed again). Raw images were automatically radiometrically calibrated to radiance units ($W \cdot sr^{-1} \cdot m^{-2}$). A 50% grey Zenith Allucore diffuse reflectance standard (SphereOptics GmbH, Herrsching, Germany) and a dark reference (0%) were recorded prior to imaging samples. Both references were used to correct for uneven illumination over the field of view. Calibrated images were exported in Envi format for further analysis using Evince software (Version 2.7.11; Prediktera AB, Umeå, Sweden).

2.5.2. Direct injection ion mobility spectrometry-mass spectrometry (DI-IMS-MS) analysis of leaf samples

Each milled, dried leaf sample was extracted in duplicate using an acetonitrile-water mixture as described by Mabizela et al. (2020) and aliquots were stored at –18 °C until DI-IMS-MS analysis according to Masike et al. (2022). The aliquots were defrosted, centrifuged, transferred to high-pressure liquid chromatography (HPLC) vials and 2 μ L of each sample injected directly into a solvent stream (50% acetonitrile, 0.1% formic acid; flow rate, 0.25 mL/min), using a Waters Accuracy ultra-high pressure liquid chromatograph (UHPLC), coupled to a Synapt G2 QTOF MS (Waters, Milford, USA). The equipment was controlled by MassLynx v.4.1 software (Waters). Data were acquired in the ion mobility scan mode (150 – 1500 amu). The ion source was an electrospray ionisation (ESI) unit, which was first operated in the positive mode and then in the negative mode with a repeated run. Mass calibration was performed using a sodium formate solution and leucine enkephalin was used as the lock spray solution. Operating

conditions were as follows: capillary voltage, 2.5 kV; sampling cone voltage, 15 V; source temperature, 120 °C; desolvation temperature, 275 °C; desolvation gas flow (N_2), 650 L/hr; cone gas flow (N_2), 50 L/hr. The wave velocity for ion mobility was set at 907 m/s and wave height at 30.2 V.

2.6. Targeted analysis of leaf composition

2.6.1. Proline accumulation

The proline content of the leaves was determined according to a slightly modified version of the method of Abraham et al. (2010). The frozen leaf samples (0.1 g) were ground using a mortar and pestle and homogenised in 0.5 mL of 3% (w/v) sulphosalicylic acid. Thereafter, 100 μ L of each homogenate was combined with 100 μ L of 3% sulphosalicylic acid, 200 μ L of glacial acetic acid and 200 μ L of an acid-ninhydrin buffer consisting of ninhydrin (1.25 g), glacial acetic acid (30 mL) and 6 M orthophosphoric acid (20 mL). The reaction mixture was heated by placing the tubes in a boiling water bath for 60 min whereafter they were cooled to room temperature in an ice bath to terminate the reaction. For extraction of the chromophore, 1 mL of toluene was added and the samples were thoroughly mixed by vortexing. After separation of the two layers, the chromophore-containing toluene was aspirated from the aqueous phase. After warming to room temperature, its absorbance was read at 520 nm against a toluene blank using a 10 mm quartz glass cuvette and a UV–visible spectrophotometer (Ultrospec 2100 pro, Amersham Biosciences, Waltham MA, USA). The proline concentration was quantified using an L-proline standard curve and calculated on fresh mass basis (μ moles/g of FM).

2.6.2. Total carbohydrates (TC) content

The carbohydrates were extracted according to the method of Kritzinger (2014), with slight modifications. Briefly, 0.1 g of the milled, dried leaves was accurately weighed (4 decimals) into 13 mm glass tubes, 4 mL of 80% ethanol was added to each tube and the content mixed using a vortex mixer. The tubes were placed in heating blocks at 80 °C for 30 min where after the tubes were removed and cooled to room temperature. The samples were centrifuged (4000 g) for 4 min at 20 °C and the supernatants decanted into 20 mL savant glass tubes. The ethanol extraction procedure was repeated three times and the supernatants were pooled, filtered through 0.45 μ m hydrophilic PVDF-L syringe filters (Filter-Bio, EthanolSA, Pretoria, South Africa) and stored at ± 6 °C until analysis.

The TC content of the extracts was estimated using the phenol-sulphuric acid assay (Dubois et al., 1956). The supernatant was diluted 10 times with distilled water. Following extraction, 200 μ L of each diluted extract was pipetted onto a 13 mm glass vial, and 200 μ L of a phenol solution (5 g phenol in 100 mL distilled water) and 1 mL of concentrated sulphuric acid were added, followed by vortexing until the mixture was uniform. The samples were left to cool to room temperature before analysis. The glucose standards were prepared as described for the samples, while the sample blank was prepared using distilled water instead of concentrated sulphuric acid. The absorbance of the samples and standards was measured at 480 nm using a quartz glass cuvette (10 mm path length) and a UV–visible spectrophotometer. The TC content of the leaves was calculated using the glucose standard curve and expressed as glucose equivalents on a dry mass basis (g/100 g dry mass (DM)).

2.6.3. Individual phenolic content

Duplicate samples (ca 40 mg) of the milled, dried leaves were weighed into 24 mL glass vials and extracted using an acetonitrile-water mixture (1:2, v/v) as described by Mabizela et al. (2020). Each extract was analysed in duplicate using a validated high-performance liquid chromatography diode array detection (HPLC-DAD) method for *C. subternata* (De Beer et al., 2012).

2.7. Proteomics

2.7.1. Collection of leaf samples and protein extraction

Plants were randomly selected between two technical replicates. The top part (20 cm) of a shoot from each of eight plants, representing a biological replicate, was removed, pooled and frozen immediately in liquid nitrogen. The samples were stored at -80°C until protein extraction. All analyses were made using three biological replicates per treatment.

The protein content of the leaves was determined using a method by Xu et al. (2008) with minor modifications. Briefly, 0.05 g of polyvinylpyrrolidone (PVPP) was added to 0.2 g of a leaf sample, which was then ground to a fine powder in liquid nitrogen using a mortar and pestle. Protein was precipitated by adding 2 mL of 10% trichloroacetic acid/acetone buffer, followed by centrifugation at 13 000 g for 3 min at 4°C . The resulting pellet was washed three times with 80% (v/v) ice-cold acetone and centrifuged at 13 000 g for 3 min at 4°C between each wash. The pellets were air-dried for an hour at room temperature and re-suspended in a phenol-sodium dodecyl sulphate (SDS) buffer (30% sucrose, 2% SDS, 0.1 M tris(hydroxymethyl)amino-methane (Tris)-HCl, pH 8.8, 5% β -mercaptoethanol) (ratio 1:1, v/v). They were vortexed for 5 min, incubated for 10 min and then centrifuged at 13 000 g for 15 min at 4°C . The supernatant was removed and 1 mL of 0.1 M ammonium acetate in 80% methanol was added to the homogenate and incubated overnight at -20°C . The supernatant was discarded, and the pellet was washed with 1 mL of 80% (v/v) ice-cold acetone and air-dried at room temperature for 60 min before re-suspended in urea buffer (9 M urea, 2 M thiourea and 4% (3-(3-cholamidopropyl) dimethylammonio)-1-propanesulfonate (CHAPS) for at least 60 min while vortexing vigorously at room temperature. The supernatant (total soluble proteins) was collected and the protein concentration was determined according to Bradford (1976), using bovine serum albumin (BSA) as a standard.

2.7.2. Two-dimensional polyacrylamide gel electrophoresis (2D-PAGE)

An aliquot of the supernatant containing an equivalent of 100 μg protein extract (based on the Bradford assay) was mixed with DE-streak rehydration solution (Bio-Rad) and made up to a final volume of 125 μL with urea lysis buffer. Samples were loaded onto a re-swelling tray and the immobilised pH gradient (IPG) strip (7 cm long, pH range 3–10) was placed on top of the sample, avoiding the formation of air bubbles. The strip was overlaid with mineral oil to prevent evaporation of the sample and allowed to passively rehydrate for 12 h at room temperature. After rehydration, the IPG strips were rinsed in distilled water, blotted on tissue paper to remove excess water and each placed on a focussing platform, with the gel side facing downwards. The strips were overlaid with mineral oil and focused on the isoelectric focusing (IEF) program according to the manufacturer's guide (Bio-Rad) using the following conditions: 250 V for 15 min, 4000 V for 1 h and finally, 4000 V at 12 000 V/h.

After IEF, the IPG strips were incubated for 15 min gel side up in re-swelling tray channels, containing 2 mL of equilibration buffer [6 M urea, 2% (m/v) SDS, 375 mM Tris-HCl, pH 8.8, 20% (v/v) glycerol and 0.01% bromophenol blue], containing 2% (m/v) dithiothreitol (DTT). This was followed by 2.5% (w/v) iodoacetamide (IAA) for another 15 min with gentle agitation at room temperature to alkylate the proteins. The equilibrated strips were placed onto 12% SDS-polyacrylamide and overlaid with 1% agarose. Electrophoresis in the second dimension was performed at a constant current of 100 V for 90 min until the bromophenol blue dye (indicator dye) reached the bottom of the gel. The gels were stained with Coomassie Brilliant Blue (CBB) for 3 h, then de-stained with a mixture of 10% (v/v) methanol, 10% (v/v) acetic acid and 80% (v/v) distilled water until the protein versus the background ratio was appropriate for visualisation.

2.7.3. Gel image analysis

Two-DE gel images were obtained using the Molecular Imager PharosFX Plus System (Bio-Rad) and the position of each individual protein was evaluated with PDQuest™ Advanced 2-D analysis software (version 8.0.1) (Bio-Rad) (Supplementary information, Fig. A3). The gels were normalised with the aid of the local regression model compensating for gel-to-gel differences in spot quantities due to non-expression related variations. Before differential protein expression was done, spots were manually edited using the consensus tool to obtain spot expression consensus across all biological replicates in the treatment groups. The amount of protein in a spot was expressed as the volume of that spot, defined as the sum of the intensities of all the pixels that make up the spot. The level of significance for the differentially expressed protein spots was set as the default (90%) in the software. Protein spots of interest were manually picked using pipette tips (QSP Certified RNase & Dnase free tips) and acetonitrile was added to the collected spots and stored at -80°C .

2.7.4. In-gel trypsin digest

The protein was reduced by rehydrating the gel pieces in 2 mM tris (2-carboxyethyl)phosphine hydrochloride (TCEP), made up in 25 mM ammonium bicarbonate (AmBic), and agitating at room temperature for 15 min. Excess liquid was removed, and this was succeeded by alkylating the gel plugs in 20 mM IAA, made up in 25 mM AmBic, and incubating them in the dark at room temperature for 30 min. After alkylation, the gel plugs were washed three times with 25 mM AmBic at room temperature for 15 min with agitation. Excess liquid was removed, and the gel pieces were dehydrated using vacuum centrifugation. The protein was digested by rehydrating the gel pieces in 0.02 mg/mL trypsin (Promega PRV5111) made up in 50 mM AmBic, ensuring that the gel pieces remained covered in the solution once rehydrated. The gel pieces were incubated on ice for 60 min whereafter the excess liquid was removed before being covered with 50 mM AmBic and digested overnight at 37°C . After digestion, the supernatant was transferred to a new LoBind tube (extract 1). The gel pieces were re-suspended in 0.1% trifluoroacetic acid and incubated for 60 min at 37°C . The excess liquid was removed and added to the first extract. Samples were dried by vacuum centrifugation and thereafter re-suspended in Millipore water. Samples were dried again by vacuum and re-suspended in a 0.1% formic acid-2% acetonitrile mixture made up in analytical grade water for liquid chromatography with tandem mass spectrometry (LC-MS/MS) analysis.

2.7.5. Protein identification by LC-MS/MS analysis

LC-MS/MS analysis was conducted using a Q-Exactive quadrupole-Orbitrap mass spectrometer coupled to a Dionex Ultimate 3000 nano-UPLC system. Data were acquired using Xcalibur v4.1.31.9, Chromeleon v6.8 (SR13), Orbitrap MS v2.9 (build 2926) and Thermo Foundations 3.1 (SP4). Peptides were dissolved in 0.1% formic acid-2% acetonitrile and loaded on a C18 trap column (PepMap100, 9027,905,000, 300 $\mu\text{m} \times 5 \text{ mm} \times 5 \mu\text{m}$). Samples were trapped onto the column and washed for 3 min with the formic acid-acetonitrile mixture before the valve was switched and peptides eluted onto the analytical column. Chromatographic separation was achieved on a Waters nanoEase (Zenfit) M/Z Peptide CSH C18 column (186,008,810, 75 $\mu\text{m} \times 25 \text{ cm} \times 1.7 \mu\text{m}$). The solvent system consisted of solvent A (0.1% formic acid in LC-grade water), and solvent B (0.1% formic acid in acetonitrile). The multi-step gradient for peptide separation was generated at 300 nL/min: 0 – 27 min, 5 – 30% solvent B; 27 – 32 min; 30 – 80% solvent B; 32 – 42 min, 80% solvent B; 42 – 45 min, 5% solvent B. To ensure carryover did not occur between runs, a wash step was added at the end of each run which comprised a gradient change of 5 – 80% solvent B in 7 min and was then held at 80% solvent B for 10 min before returning to 5% solvent B and equilibrating the column for 15 min. Data acquisition was done using Proxeon stainless steel emitters (Thermo Fisher TFES523). The mass

spectrometer was operated in positive ion mode with a capillary temperature of 320 °C. The applied electrospray voltage was 1.95 kV.

2.8. Descriptive sensory analysis of herbal tea

Preparation of the hot water infusions of the 'tea bag' fraction, training of the panel and evaluation of the samples were conducted as described in detail by Mabizela et al. (2020). Briefly, 12 female assessors with extensive experience in descriptive sensory analysis (DSA) of fermented honeybush tea evaluated 21 samples, organised with three samples/block, over a period of two days. The sample order was completely randomised over the seven blocks and to prevent panel fatigue assessors were allowed a 10 min break between consecutive blocks. Each sample was evaluated once.

2.9. Data analysis

2.9.1. Relative water content, leaf composition (targeted) and descriptive sensory analysis data

Analysis of variance (ANOVA), with drought stress treatments as a factor, was performed on the data using the General Linear Model procedure of SAS® software version 9.4 (SAS Institute Inc., Cary, NC, USA). The Shapiro-Wilk test was used to test for deviation from normality (Shapiro and Wilk, 1965). Fisher's least significant difference was calculated at the 5% level to compare treatment means (Ott, 1998). Prior to ANOVA, the DSA data were pre-processed to test for panel reliability by applying a model that includes panellist, sample effects and interactions (Næs et al., 2010) using SAS software. The residuals were tested for deviation from normality using the Shapiro-Wilk test. Outliers were removed when the standardised residual for an observation deviated with more than three standard deviations from the model value.

2.9.2. NIR-HSI analysis data

Each hypercube (384 × 284 × 288) was unfolded into a two-dimensional matrix. The pixels corresponding to the background and sample cup on the image were removed to select only the spectra of the region of interest. The average absorption spectrum for a technical replicate of a sample was calculated and the total of 63 spectra ($n = 3$ treatments × 7 biological replicates × 3 technical replicates) were used for the analysis. Principal component analysis (PCA) was performed to explore the spectral data (Wold et al., 1987). The spectra were pre-processed to correct for scatter using the Standard Normal Variate (SNV) method (Barnes et al., 1989), centred and analysed by the ANOVA-simultaneous component analysis (ASCA) method (Jansen et al., 2005) to determine whether treatment affected the leaf chemical composition.

2.9.3. DI-IMS-MS analysis data

The MassLynx raw data were converted to the mzML data format, and uploaded and analysed using the cloud-based informatics software, XCMS Online (<https://xcmsonline.scripps.edu>). Briefly, the XCMS processing parameters were as follows: matchedFilter for feature detection (with $\Delta m/z$ of 5 ppm, minimum peak width 5 s and maximum peak width 20 s), and obiwarp for retention time (RT) correction. The chromatogram alignment parameters were bw of 5 s (allowable RT deviations), minifrac of 0.5 (minimum fraction of samples necessary in at least one of the sample groups for it to be a valid group) and m/z width of 0.025 (width of overlapping m/z slices to use for peak density chromatograms and grouping peaks across samples).

Data of dimensionality (42 × 432) consisted of variables presenting data collected for 3 treatments × 7 biological replicates × duplicate extraction ($n = 42$) in negative (1–157) and positive (158–432) mode. The data were power transformed (power = 0.2) and normalised using the vsn method (Rabatel et al.,

2019). The ASCA method was used to determine whether treatment affected leaf composition.

2.9.4. Proteomics data

A database interrogation was performed using Byonic Software v2.6.46 (Protein Metrics, USA). The soybean (*Glycine max*; family Fabaceae) reference proteome sourced from UniProt (www.uniprot.org, database Uniprot_ref_Soybean_Glyc-hispida_3847_09122019) (details of search parameters are available as Supplementary information, Table A1) database was used to match peptide fragments resulting from the MS/MS data, as well as to identify proteins according to their criteria. The precursor tolerance was 7 ppm, and the fragment tolerance was 20 ppm. The maximum number of missed cleavage was two, with the protein false discovery rate (FDR) cut-off of 1% and peptide spectrum was 0.0%. A target protein with the best score ≥ 300 was considered significant. The multi-step gradient for peptide separation and mass spectrum data acquisition details are available as Supplementary information (Table A2 and Table A3, respectively).

3. Results

3.1. Relative water content (RWC)

Changes in the RWC of the leaves due to the different treatments are depicted in Fig. 1. The drought treatments had a significant effect ($p < 0.05$) on the RWC of leaves. The RWC of the plants ranged from 95 to 98% at the start of the trial (day 0) and ranged from 97 to 98% for the control plants for the duration of the trial. These levels were significantly higher than those of moderately-stressed (MS) and severely-stressed (SS) plants. The RWC of MS plants decreased gradually. Furthermore, the RWC of SS plants decreased to 87% after 4 days and decreased progressively thereafter, reaching the lowest value (47%) at the end of the treatment period (day 11).

3.2. Untargeted analysis of leaf chemical composition

The results of the ASCA analysis of both the NIR-HSI and DI-IMS-MS data sets give evidence that the drought stress treatments significantly ($p < 0.01$) affected leaf chemical composition as indicated by the null distribution of the sum of squares obtained from the randomisation test and the observed sum of squares for the respective data sets (Figs. 2a and 3a). Projection of the group means and individual samples on the plane defined by PC1 and PC2 show three separate groupings, according to treatment (Fig. 2b and Fig. 3b). The NIR-HSI data produced a large number of loadings (variables) that were significant (Fig. 2c), mostly at variable numbers < 170 (< 1828 nm), while six significant variables (28, 33, 169, 194, 287, 427) were identified for the DI-IMS-MS data (Fig. 3c). Further research is needed to identify the plant constituents responsible for the differences.

3.3. Targeted analysis of leaf composition

Accumulation of proline in the leaves depended on the treatment (Fig. 4), varying from no effect for the WW treated leaves ($p \geq 0.05$) to a significant increase ($p < 0.05$) to between 21.65 and 38.95 $\mu\text{moles/g}$ FM in the SS treated leaves from day 4 until day 10. In contrast, the proline content of MS treated leaves increased up to 5.2 $\mu\text{moles/g}$ FM at day 10.

Both the total carbohydrate and individual phenolic compound content of the leaves were not significantly ($p \geq 0.05$) affected by drought stress. The content of the individual phenolic compounds is available as Supplementary information (Table A4).

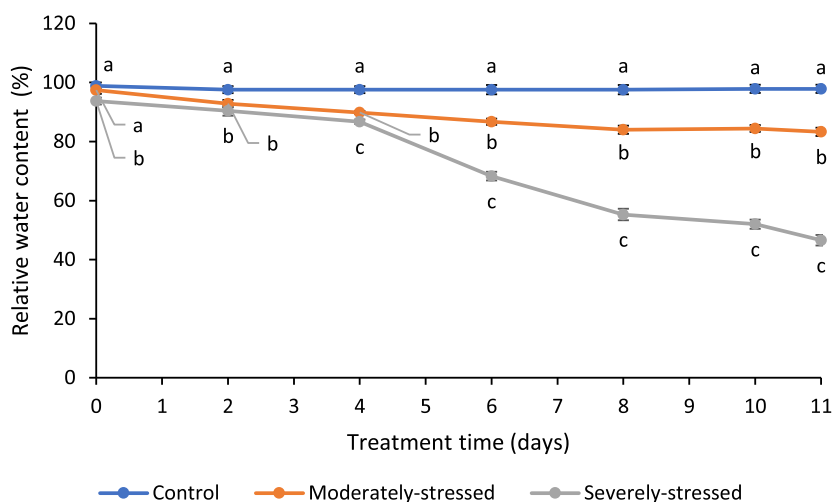


Fig. 1. Changes in the RWC of well-watered (control) and drought-stressed (moderately-stressed and severely-stressed) *Cyclopia subternata* plants, stressed for ten days, harvested every second day. Means at the same time point with the same letters are not significantly different ($p < 0.05$). Error bars indicate the standard error between the means.

3.4. Proteomics analysis

3.4.1. Two-dimensional electrophoresis analysis of stress-responsive proteins in *Cyclopia subternata* leaf samples

The optimum content of *C. subternata* proteins was 100 μ g, resolved in 7 cm IPG strips of pH range 3–10 and 12% (v/v) SDS PAGE gels. From the analysis of differential protein expression between the treatments, a total of 114 protein spots exhibited significant differences. The three biological and technical replicates analysed for each treatment are available in the Supplementary information (Fig. A2).

3.4.2. Identification of stress-responsive proteins of *Cyclopia subternata* using LC-MS/MS

Briefly, 27 differentially accumulated proteins (DAPs) (Fig. 5) were selected, excised and identified using LC-MS/MS. Table 1 presents detailed information (protein accession number, Byonic score, total number of amino acids, peptide spectrum match, etc.) concerning these protein spots. Since the honeybush proteome has not been quantified, the proteome of the closely related crop from the Fabaceae family (*Glycine max*) was used as a proteome reference source. The log probability (≥ 1) and Byonic (≥ 300) score determined the significance of the identified proteins. Seventeen DAPs were up-regulated and another 10 were down-regulated. However, from the 27 DAPs that were selected, only 24 (17 up-regulated; 7 down-regulated) were successfully identified, 13 DAPs of which produced significant results based on their Byonic scores (≥ 300). Three of the 27 DAPs were unknown due to the lack of database matches. Compared to the WW treatment, the MS treatment up-regulated 11 DAPs (2, 6, 8, 11–14, 22, 24, 25) and down-regulated 16 DAPs (3, 4, 5, 7, 9, 10, 15–21, 23, 26, 27). Furthermore, the SS treatment up-regulated 14 DAPs (1, 2, 3, 5, 6, 10–14, 19, 21, 22, 25) and down-regulated 13 DAPs (4, 7–9, 15–48, 20, 23, 24, 26, 27) compared to the WW treatment (Table 1). The identified proteins were classified according to their putative functions, i.e. photosynthesis proteins, defence proteins, carbohydrate and energy metabolism proteins, stress response-related proteins, ATP interconversion proteins and signal transduction proteins (Fig. 6).

3.5. Sensory analysis of herbal tea

The sensory attributes and thus the sensory profile of the herbal tea product were not significantly affected by drought stress as shown by ANOVA (Supplementary information, Table A5).

4. Discussion

4.1. Relative water content of leaves

The RWC, calculated as the percentage of water present in the leaf relative to the total volumetric water that the leaf can hold at full turgor (Blum, 2011), is a key indication of water stress in leaves and is directly linked to soil water content (Xu et al., 2021). This parameter is important as it has a significant effect on photosynthesis (Podda et al., 2019). Drought stress hampered *C. subternata* growth by decreasing the RWC. A decline in RWC of drought-stressed *C. subternata* leaves is a common observation, depicting the drought sensitivity of the plant. This is in accordance with drought stress studies on other plants (Kabbadj et al., 2017; Amnan et al., 2022). For instance, a low leaf RWC was observed for *Pandanus* (Amnan et al., 2022) and Ethiopian red pepper plants (Wassie et al., 2023) subjected to drought stress. Furthermore, the slight decrease in the RWC of the MS treated plants may indicate that this *Cyclopia* species is tolerant to mild-to-moderate water stress. The change in the RWC of *C. subternata* leaves indicates that RWC may be used to show the level of water stress in honeybush plants. This can be employed in crop improvement programmes, as well as efficient management practices for honeybush cultivation under drought stress conditions.

4.2. Untargeted analysis of leaf chemical composition

First, an untargeted chemical analysis approach was followed to determine whether treatment affected the composition of the leaves. NIR-HSI was used because it is a rapid method which collects data with high spatial and spectral resolution and could be applied directly to the finely milled, dried leaf samples without further preparation. This method has been applied to a large variety of plant materials including *Camellia sinensis* teas to indicate compositional differences due to various treatments (as reviewed by Mao et al., 2022). In the present study, significant differences were detected between the *C. subternata* leaf samples of the plants subjected to different water regimes. Significant variables identified using NIR-HSI correspond to wavelengths < 1828 nm. The molecular bonds which respond in this spectral region include mainly the first and second overtones of O–H, N–H and C–H stretching vibrations (Lin and Sun, 2020). These bonds are typical of organic compounds such as proteins and carbohydrates (Manley, 2014). Following NIR-HSI, extracts of the leaf samples were analysed by DI-IMS-MS. From this data set, six variables contributing to the differentiation between the treatments

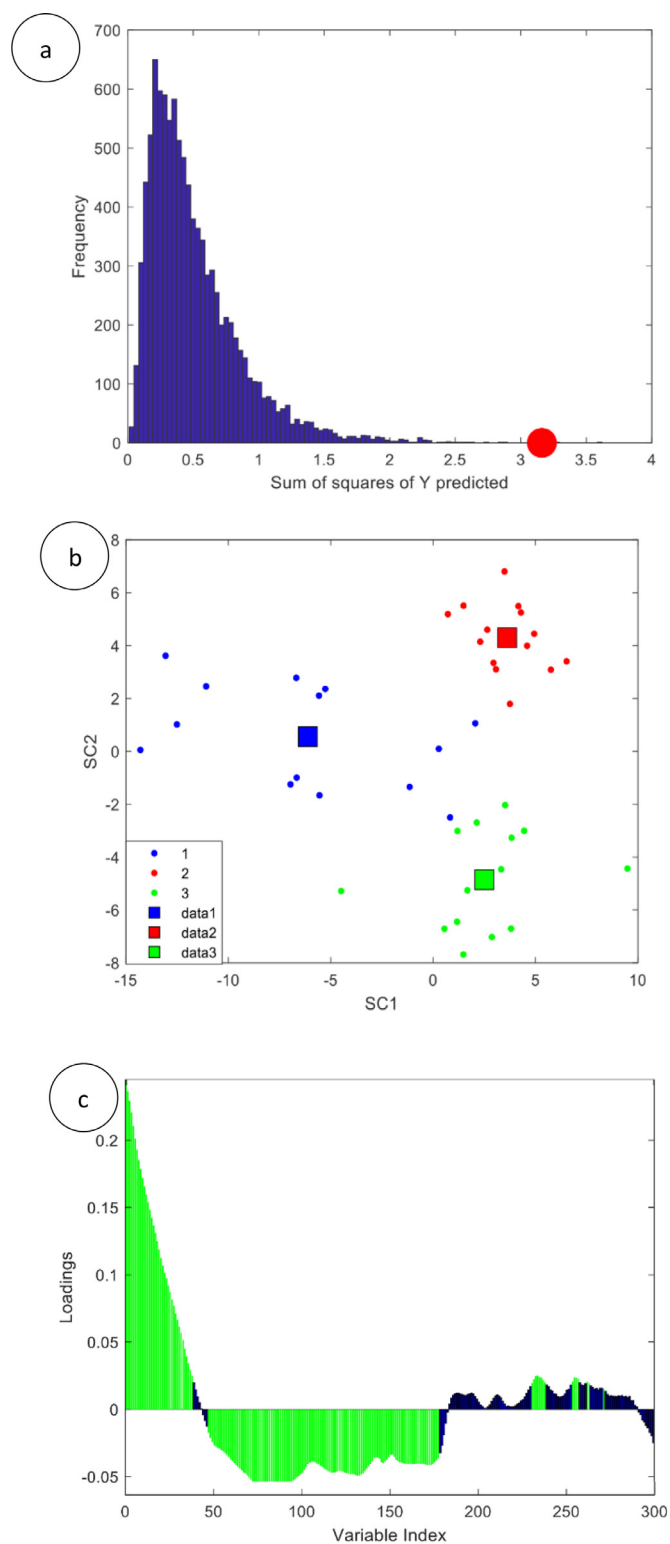


Fig. 2. ASCA results for NIR-HSI data of *Cyclopia subternata* plants, subjected to three water treatments (control, moderately-stressed (MS) and severely-stressed (SS)), for ten days: (a) null distribution of the sum of squares for treatment obtained based on randomisation test (10,000 runs) and the observed sum of squares (marked with a red circle), (b) scores plot of PC1 and PC2 with three groupings representing the treatments (blue = well-watered (control), red = moderately-stressed and green = severely-stressed), and (c) loadings plot of PC1 and PC2s (with green indicating significant variable numbers, $p < 0.05$).

could be identified, providing further confirmation that treatment affected the leaf composition. Further studies are required to identify the leaf constituents corresponding to these variables.

4.3. Targeted analysis of leaf chemical composition

Proline plays an important role in stress tolerance, and its accumulation is the first response of plants to reduce injury to cells when exposed to a water deficit (Mahmoud et al., 2020). Not only does proline act as an osmolyte (Tonhati et al., 2020), but it may also play a role in the scavenging of reactive oxygen species (ROS) and other free radicals (Alvarez et al., 2022). In the present study, the proline content of *C. subternata* leaves during the severe drought stress period increased more than 40-fold compared to the control. Proline accumulated to a much higher level under these conditions, indicating that it might act as an osmoprotectant (Spormann et al., 2023). Other protective mechanisms of proline include acting as a chemical chaperone and direct scavenging of ROS (Mattioli et al., 2020). In accordance with Wang et al. (2016a), the increase in the proline content of *C. subternata* leaves may further indicate that the generation of ROS in cells was lowered, and toxic effects in the plant were reduced, as confirmed by the proteomics results in this study. A high proline content in Ethiopian red pepper (Wassie et al., 2023), *Amaranthus* species (Slabbert and Kruger, 2014) and *Achillea* species (Gharibi et al., 2016) following drought stress has also been reported. Furthermore, Ainhout et al. (2001) noted that when the leaf water potential in *Halimium halimifolium* declined to -2.9 MPa during water deficit, a significant increase in proline concentration was observed. The accumulation of proline observed for *C. subternata*, possibly also reducing cell stress and damage, represents an important adaptive response, thereby improving the tolerance and survival of the plants during drought stress.

It is a general hypothesis that water deficit can lead to an increase in carbohydrate and phenolic content by altering biochemical processes. However, in the present study, these compositional parameters were not significantly affected by the drought stress treatments, probably due to the relatively short treatment period. *Aspalathus linearis*, another fynbos legume plant, showed a decline in its maximum photosynthetic rate as well as a 50% decline in growth rate after being stressed for six weeks (Lotter et al., 2014).

4.4. Sensory analysis of the herbal tea

Sensory analysis of the infusions of *C. subternata* herbal tea showed that drought stress also did not negatively affect their aroma, taste and astringency. Studies on *Camellia sinensis* plants showed that drought stress affects the content of constituents directly related to taste and aroma (i.e. polyphenol and aroma compounds, respectively) (Qian et al., 2018) and subsequently product quality (Ahmed et al., 2019). Although the composition of *C. subternata* differs from that of *C. sinensis*, the lack of effect for *C. subternata* is, once again, likely due to the short drought stress period.

4.5. Proteomics analysis

Understanding how *C. subternata* responds to drought stress at the molecular level is vital to improve the quality and production of honeybush plants. In this study, about a third of the identified proteins were detected in multiple spots with different molecular masses and isoelectric points (pIs), implying the existence of isoforms and post-translational modifications. The putative amplifications for identified proteins in drought-stressed plants are identified below. The largest DAP groups were proteins involved in photosynthesis (25%), followed by those involved in defence (17%), carbohydrate/energy metabolism (17%) and stress-response (17%) (Fig. 6), suggesting their important roles in the response of the plant to drought stress conditions. However, as seen with most biochemical processes, proteins are not limited to one functional group, e.g. a stress-response protein may also be regulated during a defence-response

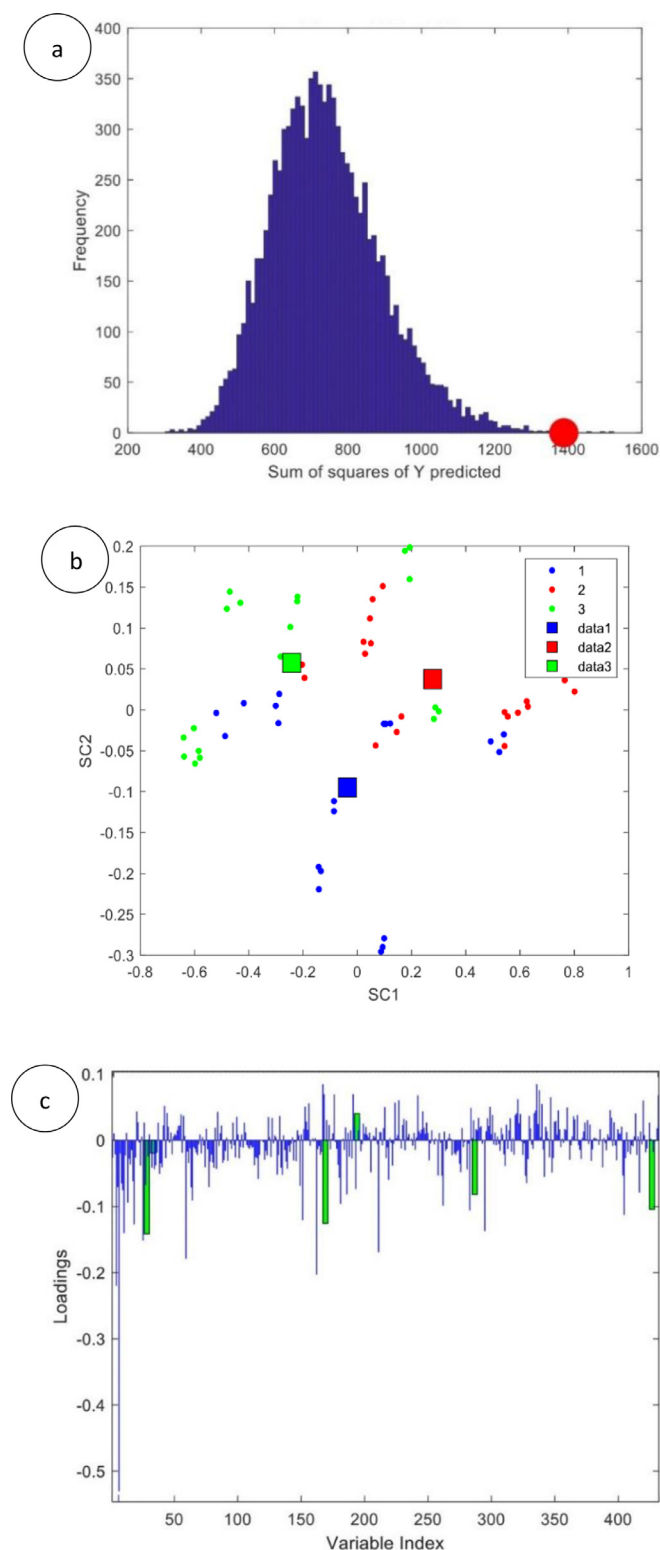


Fig. 3. ASCA results for DI-IMS-MS data of *Cyclopsia subternata* plants, subjected to three water treatments (control, moderately-stressed (MS) and severely-stressed (SS)), for ten days: (a) null distribution of the sum of squares for treatment obtained based on randomisation test (10,000 runs) and the observed sum of squares (marked with a red circle), (b) scores plot of PC1 and PC2 with three groupings representing the treatments (blue = well-watered (control), red = moderately-stressed and green = severely-stressed), and (c) loadings plot of PC1 and PC2 indicating six significant variables ($p < 0.05$), indicated by green bars.

event. Only proteins that were identified in the largest DAP groups will be discussed in the following sections.

4.5.1. Modulation of photosynthesis-related proteins during drought stress

Photosynthesis and photorespiration are important sources of energy in plant cells. They are, nevertheless, vulnerable to drought stress (Wang et al., 2022a). Drought stress inhibits photosynthetic activity primarily through stomatal closure, resulting in lower carbon fixation and a decreased electron transport system (Chen et al., 2023; Sherin et al., 2022).

Drought stress impacted photosynthesis and triggered the antioxidant defence system in *C. subternata* leaves. Most of the identified proteins are those involved in photosynthesis, including ribulose-1,5-bisphosphate carboxylase/oxygenase (Rubisco) large unit, Rubisco activase, photosystem II (PSII), light-harvesting chlorophyll a/b-binding proteins (LHCB), carbonic anhydrase and glutamine synthetase (GS), are involved in photosynthesis mechanisms, such as the Calvin cycle, electron transport chain and light-harvesting (Ali et al., 2023; Goharrizi et al., 2022; Shanker et al., 2022; Singh et al., 2022). Of the six photosynthetic proteins, four proteins (Rubisco activase, LHCB, carbonic anhydrase and GS) were up-regulated in both MS and SS treated plants, furthermore, two proteins had decreased in abundance or were absent under SS conditions, while they did not show any significant change or were up-regulated under MS conditions (Table 1).

Rubisco is a key enzyme of the Calvin cycle, catalysing the fixation of atmospheric carbon from CO_2 to the sugar phosphate, ribulose-1,5-bisphosphate (Chen et al., 2023). It was up-regulated under SS conditions but down-regulated under MS conditions. Similar findings were reported by Wang et al., 2022a) where the activity of Rubisco was significantly higher during drought stress compared to short-term drought or control conditions. Drought is an example of abiotic stress that slows down photosynthesis by interfering with cell homeostasis, impacting the electron transport chain, photophosphorylation, soluble proteins, proteins in thylakoid membranes, and photosynthetic pigments (Brestic and Allakhverdiev, 2022). Based on the findings for the relative abundance of the proteins, the impact of abiotic stress as a result of drought stress could be established in the current study.

The photosynthetic machinery consists of photosystem II (PSII), cytochrome b6f complex (Cytb6f), and photosystem I (PSI) (Kornienko et al., 2018). PSII is a multi-component pigment-protein complex that is found in the thylakoid membranes of oxygenic photosynthetic organisms, including plants (Sasi et al., 2018). The water molecule is broken during photosynthesis by PSII, which then delivers electrons to PSI via the plastoquinone pool. Plastocyanin then transfers electrons from Cytb6f to PSI (Yang et al., 2022). However, in conditions of drought stress, PSI electrons can be transported to oxygen, producing ROS (Ye et al., 2015). PSII complexes were shown to be less abundant in SS treated *C. subternata* plants, suggesting that the drought stress experienced by the plants caused damage to thylakoid protein complexes. These results are comparable with those of Bashir et al. (2021). Furthermore, the decrease in PSII in MS treated plants may suggest that there was a decrease in photosynthesis under mild to moderate drought stress conditions. This may lead to plants absorbing more light than needed for photosynthetic carbon fixation, which may cause an increase in ROS production (Muneer et al., 2014) in *C. subternata*.

This study further demonstrated that light reaction was strongly affected by drought stress, because proteins related to light reactions, i.e., LHCB, increased in abundance under drought stress conditions compared with well-watered conditions. This may contribute to the optimisation of light energy capture, protection against excess light and maintenance of photosynthetic efficiency under water-limited conditions (Vayghan et al., 2022). These findings are in agreement with those on tolerant *Zea mays* hybrids (Bashir et al., 2021). Additionally, Mehari et al. (2021) reported an increase in LHCB genes (*Gh_D10G2385* and *Gh_D05G0860*) of *Gossypium hirsutum* leaf tissue

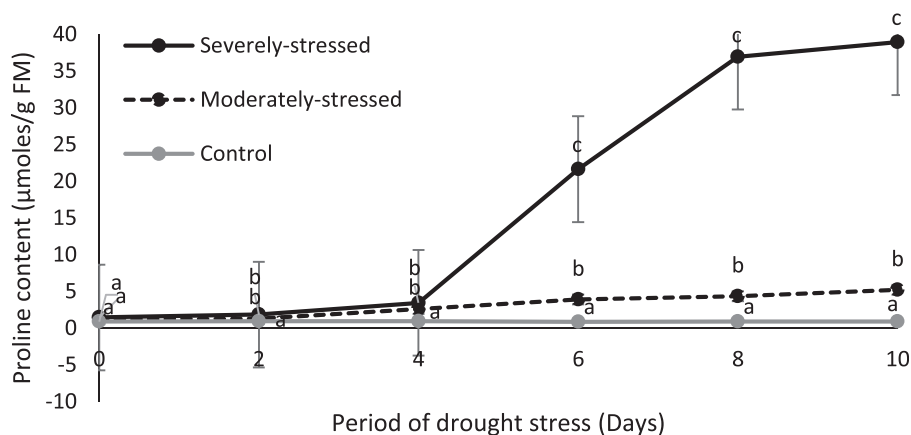


Fig. 4. Changes in the proline accumulation in the leaves of *Cyclopia subternata* plants, subjected to three water treatments (control, moderately-stressed (MS) and severely-stressed (SS)), for ten days, collected every second day. Means with the same letters are not significantly different ($p < 0.05$). Error bars indicate the standard error between the means.

under drought stress. Furthermore, the increased abundance of this photosynthetic protein in *C. subternata* could be a potential target for use in transgenic studies, potentially improving the photosynthetic efficiency of the plant under abiotic stress.

Carbonic anhydrase was up-regulated in *C. subternata* leaves under drought stress conditions, suggesting that carbon assimilation by Rubisco was increased. The results further explain that a high level of carbonic anhydrase in *C. subternata* leaves may have alleviated the cytotoxic concentrations of H_2O_2 during drought stress (Chang et al., 2019).

Glutamine synthetase (GS) is an important enzyme in nitrogen metabolism, catalysing the condensation reaction of glutamate and ammonia to form glutamine (Yin et al., 2022). The GS enzyme was significantly up-regulated in *C. subternata* leaves in response to

drought stress conditions, suggesting a positive effect on nitrogen metabolism, which may be true as *Cyclopia* species are legumes and thus known to fix their own nitrogen (Postma et al., 2016). This nitrogen fixation, facilitated by rhizobia, assists plants to produce their own nitrogen and has a positive effect on nutrient uptake and plant growth (Wang et al., 2022b). The function of root nodules and the growth of honeybush are directly affected when plants receive less water during the summer months. Drought also impacts on photosynthesis by lowering its rate and the level of photosynthates needed by the bacteria for nitrogen fixation (Brink et al., 2017). The proteomic findings provided evidence that the regulation of photosynthesis-related proteins in *C. subternata* during drought stress may be vital in tolerance studies on the plant.

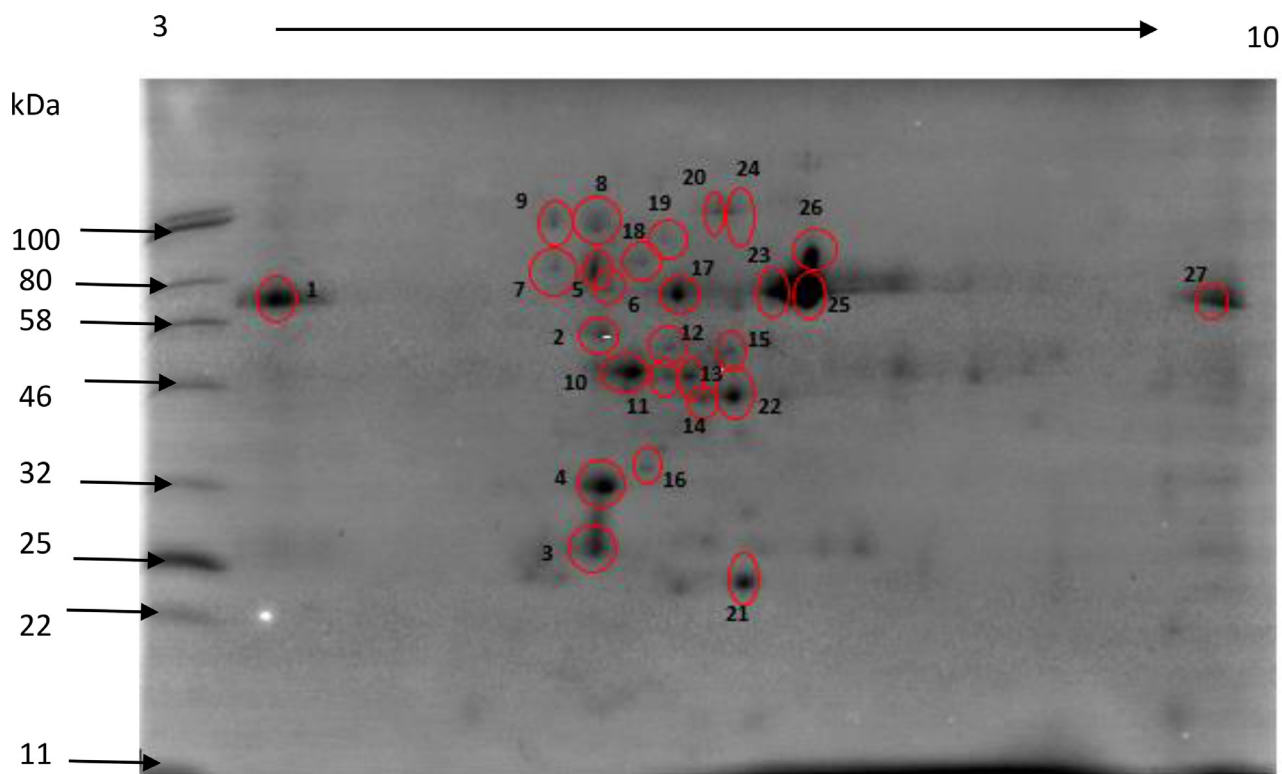
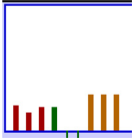
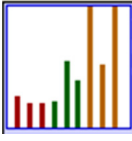
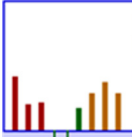
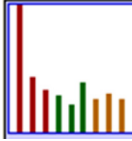
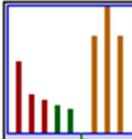
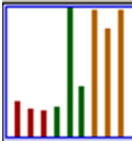
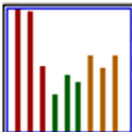
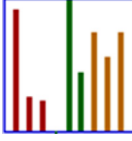


Fig. 5. Two-dimensional electrophoresis gel obtained during analysis of protein extracts from *Cyclopia subternata* leaves. The gel shows 27 annotated *C. subternata* drought stress-responsive proteins that were selected for LC-MS/MS analysis. About 100 µg of the leaf protein extract was separated by isoelectric focussing using 7 cm immobilised pH gradient strips, pH ranges 3–10 and 12% sodium dodecyl sulphate-polyacrylamide gel electrophoresis gels in the second dimension. Labels indicate drought responsive proteins, numbered from 1 to 27.

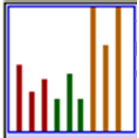
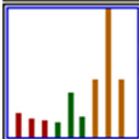
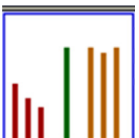
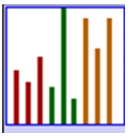
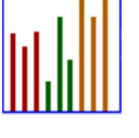
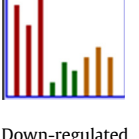
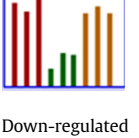
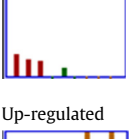
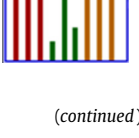
Table 1

Details of 27 differentially accumulated proteins in leaves of *Cyclopia subternata* under drought stress, listed according to their putative functions. Identification of proteins was by LC-MS/MS analysis.

Spot no.	Protein name	Function	Log probability	Byonic score	Calculated mass (M + H) ⁺	Mass error (ppm)	No. of unique peptides	No. of amino acids in protein	Expression change
1	Ribulose-1,5-biphosphate carboxylase/oxygenase (Rubisco) large unit	Photosynthesis	8.39	524	1546.736	-1.3	40	475	Up-regulated 
2	Putative disease resistance protein	Protective function	1.37	230.9	561.361	0.2	2	1307	Up-regulated 
3	Lambda-class glutathione S-transferase (GST)	ROS scavenging/defence/stress-related	1.12	147.9	1086.641	-0.3	2	239	Down-regulated 
4	ATP synthase subunit α	ATP interconversion	15.44	376.8	1612.902	-1.9	5	1070	Down-regulated 
5	Photosystem II protein D1	Photosynthesis	2.4	103.5	1459.733	-2.2	2	353	Up-regulated 
6	Phospholipid-transporting ATPase 1	ATP interconversion	1.34	307.2	763.410	-1.1	2	1106	Up-regulated 
7	pH domain-containing protein	Signal transduction	0.64	154	1317.701	0.1	2	4321	Up-regulated 
8	Chlorophyll a/b binding protein 2, chloroplastic	Photosynthesis	4.15	313.4	982.532	0.8	2	1070	Up-regulated 

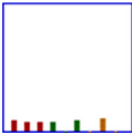
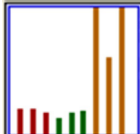
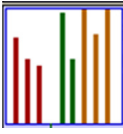
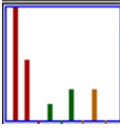
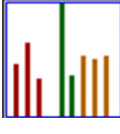
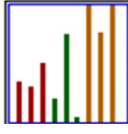
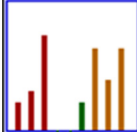
(continued)

Table 1 (Continued)

Spot no.	Protein name	Function	Log probability	Byonic score	Calculated mass (M + H) ⁺	Mass error (ppm)	No. of unique peptides	No. of amino acids in protein	Expression change
10	Chalcone synthase 5	Defence	5.02	343.2	1593.867	1.4	2	388	Up-regulated 
11	Fructose-bisphosphate aldolase	Stress response-related	6.02	385.4	1004.552	0.7	3	395	Up-regulated 
12	Phosphoglycerate kinase	Energy metabolism	8.8	349.7	1198.741	0.6	6	483	Up-regulated 
13	Glutamine synthetase	Photosynthesis	9.36	670.5	1817.857	1.5	5	356	Up-regulated 
14	Malate dehydrogenase	Photosynthesis	19	373	2016.131	-1.0	13	328	Up-regulated 
16	Lactoylglutathione lyase	Signalling pathway	7.21	480	1164.506	-0.1	5	356	Down-regulated 
17	Peroxidase	ROS scavenging/defence/stress-related	1.12	178.9	1765.033	-3.6	2	324	Down-regulated 
18	Rubisco activase	Photosynthesis	2.43	231.5	1152.714	2.8	2	478	Down-regulated 
19	UDP-sugar pyrophosphorylase 1	Energy metabolism	4.62	431.6	1259.711	0.0	4	600	Up-regulated 

(continued)

Table 1 (Continued)

Spot no.	Protein name	Function	Log probability	Byonic score	Calculated mass (M + H)*	Mass error (ppm)	No. of unique peptides	No. of amino acids in protein	Expression change
20	Zeaxanthin epoxidase, chloroplastic	ROS scavenging/defence/stress-related	9.6	378.2	1182.579	0.4	2	667	Down-regulated 
21	Carbonic anhydrase	Photosynthesis	6.03	363	1235.518	-0.6	4	324	Up-regulated 
22	Inositol methyltransferase	ROS scavenging/defence/stress-related	1.39	198	1297.603	0.6	2	369	Up-regulated 
23	DNA helicase	Signal transduction	0.94	226.4	645.357	0.2	3	848	Down-regulated 
24	Phenylalanine ammonia-lyase	Defence	4.73	276.7	2179.172	1.0	2	716	Up-regulated 
25	Glucose-1-biphosphate aldenyltransferase	Energy metabolism/starch synthesis	1.32	163	1199.690	1.9	3	523	Up-regulated 
27	Tubulin alpha chain	Signal transduction	6.7	395.1	1342.639	-0.1	3	408	Down-regulated 

Log probability = the log p-value of the peptide spectrum match (PSM). PSM ≥ 1 for a hit to be significant; **Byonic score** = primary indicator of PSM correctness. A score of ≥ 300 is considered to be a significant hit (Bern and Kil, 2011; Khoza et al., 2019); **Calculated mass** = the computed M + H precursor mass for the PSMs; **Error mass** = a calculated mass error (parts per million) after correcting the observed M + H (single charged) precursor mass and the computed M + H precursor mass; **No. of unique peptides** = total number of PSMs; **No. of spectra** = total number of PSMs, including duplicate PSMs, discounting duplicates. Bar graphs shows differential expression pattern of the three water treatments and replicate number, where red = well-watered (WW), green = moderately-stressed (MS) and orange = severely-stressed (SS).

4.5.2. Regulation of defence proteins during drought stress

Protein content and quality in plants are impacted by drought stress. Under adverse environmental conditions, plants synthesize enormous quantities of ribosomal and chaperone proteins (Li et al., 2020). All of these proteins play crucial roles in maintaining correct protein production, folding denatured proteins, and disaggregation of denatured proteins, aiding in stress adaptation (Wu et al., 2022). In the present study, four proteins were identified as defence proteins, of which two were antioxidant enzymes. One of the proteins was for defence, i.e., putative disease-resistant protein, which increased

under drought stress. The other was used for activation of antioxidant defence, i.e., zeaxanthin epoxidase, which was down-regulated following drought stress. The two antioxidant enzymes were phenylalanine ammonia-lyase (PAL) and chalcone synthase 5 (CHS5).

PAL plays a role in the biosynthesis of lignins, phenolic acids and flavonoids which are secondary metabolites that play an important role in plant defence (Tolrà et al., 2020). Phenolic compounds are usually accumulated in plants under abiotic stress conditions, including water deficit (Rasool et al., 2021). PAL was increased in *C. subternata* leaves under drought stress conditions, although the level of

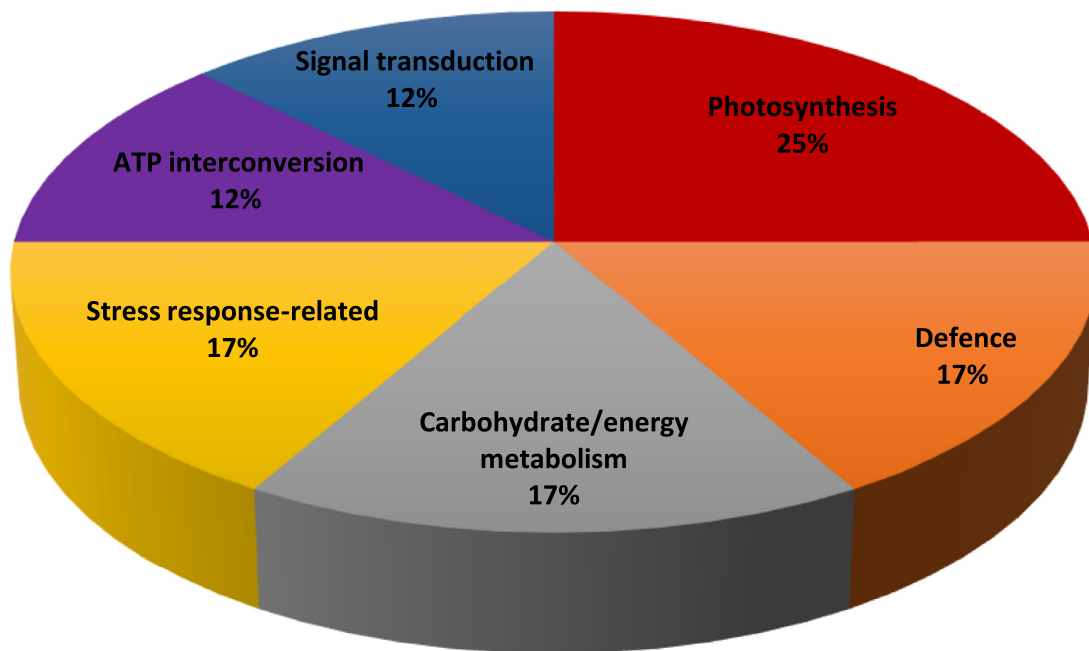


Fig. 6. A pie chart indicating the functional classification of identified proteins in the leaves of *Cyclopia subternata* plants, subjected to drought stress for ten days. The identified proteins were categorised into six groups.

accumulation of this protein was not significant (Byonic score < 300), and may explain the non-significant effect of drought stress on the phenolic content of the leaves. This may further suggest that an extended drought duration is required to stress *C. subternata* plants to such an extent that detectable changes in phenolic composition would occur.

CHS5, a key enzyme in flavonoid biosynthesis (Liou et al., 2018), was highly up-regulated (> 300 Byonic score) in *C. subternata* leaves under drought stress. This may be an indication that this enzyme is essential for its drought adaptation as demonstrated for other plants such as chilli pepper (Rodriguez-Calzada et al., 2019), Indian wheat (Singh et al., 2020) and sweet cherry (Hou et al., 2022). The upregulation of CHS5 would lead to the expectation that the biosynthesis of flavonoids in *C. subternata* leaves may be increased by drought stress, but as already noted, no detectable increase in the prominent flavonoids was observed. Naringenin, one of the first flavonoids formed in the flavonoid biosynthesis pathway (An et al., 2021) and the aglycone of several glycosides was present at low levels in *C. subternata* (De Beer et al., 2012), was reported in higher levels in strawberries under drought stress (Perin et al., 2019).

4.5.3. Responses of carbohydrate and energy metabolism proteins during drought stress

Carbohydrate metabolism in plants is a dynamic and interconnected network of pathways that ensures energy supply, carbon storage and synthesis of essential molecules for growth and development (Diniz et al., 2020). The balance between energy production and storage is crucial for plants to adapt to varying environmental conditions such as drought stress, in order to sustain their physiological processes (Bijalwan et al., 2022). In this study, proteins involved in carbohydrate metabolism including malate dehydrogenase (MDH), fructose-1,6-bisphosphate aldolase (FBA), UDP-sugar phosphorylase 1 (UGPase) and glucose-1-bisphosphate aldehyltransferase (GBA) were amongst those that were the most abundantly increased in *C. subternata* leaves, most probably due to an increased energy demand caused by drought stress. The findings are comparable to those reported by Amnan et al. (2022) where a high abundance of carbohydrate proteins was observed for *Pandanus amaryllifolius*.

MDH is an enzyme involved in the citric acid cycle (Krebs cycle or TCA cycle) and other metabolic processes in plants (Zhao et al., 2020). It catalyses the reversible conversion of malate to oxaloacetate, using NAD⁺ as a coenzyme (Nan et al., 2020). Drought stress often leads to limited photosynthesis due to reduced water availability (Bijalwan et al., 2022), and as a result, plants rely more on respiration to generate energy. In the present study, the MDH abundance in *C. subternata* leaves increased under drought stress. This increase may have facilitated the conversion of malate to oxaloacetate, providing an additional substrate for the Krebs cycle, and thus promoting respiratory activity, allowing plants to produce ATP and meet their energy demands under drought stress conditions (Zhao et al., 2020). Similar findings were reported in soybean (Wang et al., 2022b).

Fructose-1,6-bisphosphate aldolase (FBA) was up-regulated in *C. subternata* leaves under drought stress. The enzyme is involved in the glycolytic pathway in the cytoplasm, whereas it is part of the Calvin cycle in the chloroplast (Cai et al., 2022). FBA genes are involved in various important physiological and biochemical processes, including plant development, signal transduction, regulation of secondary metabolism, plant defence and response to biotic and abiotic stresses (Pirovich et al., 2021). In this study, the increase in the expression of FBA enzyme could imply the maintenance of glucose metabolism and signal transduction in *C. subternata* plants during the period of drought stress and may thus be classified as moisture/water stress-responsive marker protein in the chloroplast (Xia et al., 2022). Similar results were reported by Nazari et al. (2020) for wheat. Carrera et al. (2021) stated that the increase in FBA levels in *Arabidopsis* is indicative of an increased sucrose production in the cytosol and turnover in the vacuole. This can further be supported by the increase in UGPase and glucose 1-bisphosphate aldehyltransferase (GPT) expression in the current study.

UGPase is an enzyme that serves as a substrate for the formation of disaccharides, such as the signalling and energy transport/storage molecule sucrose or the signalling molecule, trehalose-6-P (Qin et al., 2021). Furthermore, the upregulation of UGPase in *C. subternata* leaves indicates a potential increase in carbohydrate synthesis that may modify gene expression and proteomic patterns (Decker and Kleczkowski, 2019). GPT plays a role in starch synthesis and it

catalyzes the synthesis of the activated glycosyl donor, ADP-glucose from Glc-1-P and ATP (Peredes-Flores & Mohiuddin, 2022). The up-regulation of this enzyme in *C. subternata* leaves may have contributed to enhancing starch synthesis, osmotic adjustment, altered carbon partitioning and potentially affected gene expression patterns under drought stress conditions.

4.5.4. Responses of stress response-related proteins during drought stress

Glutathione S-transferases (GSTs) play multifaceted roles in plants, including xenobiotic detoxification, antioxidant defence, hormone homeostasis, and responses to biotic and abiotic stresses (Zhunge et al., 2020). The GST activity has been reported to increase in plants under abiotic stress (Kumar and Trivedi, 2018). Moreover, expression of the GST gene, *GsGSTU8*, was highly induced after water stress by increased concentrations of abscisic acid in *Camellia sinensis* (Zhang et al., 2021). Yilmaz et al. (2023) reported an increase in GST activity in wheat under drought stress suggesting their involvement in defence against oxidative stress caused by drought. While an increase in GST activity is commonly reported under drought stress, limited research exists that specifically reported a decrease in GST activity under drought stress. Studies in wheat (Chen et al., 2004) showed a decrease in GST activity under drought stress. In the present study, the GST level in *C. subternata* leaves was increased by the SS treatment, whereas it was decreased by the MS treatment. This might be explained by the regulation of gene expression in this multigene family which is controlled by different mechanisms, and thus the inducibility of the different GST genes will differ according to the type of stress (Panara et al., 2022).

Lactoylglutathione lyase (glyoxalase I) is an enzyme that converts methylglyoxal and other 2-oxoaldehydes to their 2-hydroxy acids using glutathione as a cofactor (Chakraborty et al., 2015). Methylglyoxal is a cytotoxic compound, produced in many cellular metabolic processes, and it accumulates in plants under diverse environmental stresses (Armeni et al., 2014). Under drought stress conditions, plants often experience various physiological and metabolic changes as they adapt to limited water availability (González, 2023). In some cases, a decrease in lactoylglutathione lyase or glyoxalase I activity has been observed in plants under drought stress. A study on *Brassica napus* plants subjected to drought stress reported a reduction in glyoxalase I activity in the leaves of stressed plants (Hasanuzzaman et al., 2018). Furthermore, the abundance of lactoylglutathione lyase was decreased under drought stress conditions in the present study. This decrease may have several implications in *C. subternata* plants, such as increased methylglyoxal levels which may lead to cellular damage, as well as an increase in ROS production due to oxidative stress (Brossa et al., 2015). *Vigna radiata* plants subjected to drought stress showed a disrupted glyoxalase system (Nahar et al., 2017) which supports the result of our study.

Peroxidases (Class III) are enzymes which are crucial for plant development, defence against pathogens and response to abiotic stress (Shigeto and Tsutsumi, 2016). They are involved in various physiological processes, including lignin biosynthesis, cell wall remodelling and plant defence against pathogens (Kidwai et al., 2020). Peroxidase was down-regulated in this study in response to drought stress, which could indicate a reduction in the capacity of *C. subternata* to detoxify ROS, such as H₂O₂, leading to ROS accumulation.

Inositol methyltransferase was up-regulated in *C. subternata* leaves following drought stress. Its function is to catalyse the methylation of *myo*-inositol into *D*-ononitol, the first step in the biosynthesis of the cyclic sugar, *D*-pinitol (via the *myo*-inositol-*O*-methyltransferase (*IMT1*) gene). Dumschott et al. (2019) reported an up-regulation of *IMT1* in soybean under water deficit. *D*-Pinitol has osmoprotective properties (Ostrowski et al., 2020) and is the most abundant sugar in many Fabaceae species, including *C. subternata*. The pinitol content of

a *C. subternata* extract was more than 4 mg/100 g extract (Yoshida et al., 2020). The up-regulation of inositol methyltransferase in *C. subternata* following drought stress may indicate the importance of this enzyme in the ability of the plant to survive under this stress condition.

It is clear from the results of this study that drought-induced protein expression could contribute towards plant stress tolerance mechanisms and these proteins could thus be useful candidates for further investigation of their molecular mechanisms of action in plants, particularly honeybush during drought stress conditions.

5. Conclusions

In this study, drought stress reduced the RWC of *C. subternata* leaves. In addition, untargeted chemical analysis using NIR-HSI and DI-IMS-MS techniques revealed significant variations across drought stress treatments, however, the plant constituents responsible for these differences were not identified. Targeted chemical analysis revealed that drought stress drastically augmented the proline level of *C. subternata* leaves compared to leaves of well-watered plants, implying that proline may have acted as an osmoprotectant, protecting the plants from cell damage and enhancing survival during drought stress. Contrary to expectations, drought stress treatments had no effect on the individual phenolic compound and total carbohydrate content of *C. subternata* leaves, as well as the sensory profile of the herbal tea. These findings imply that *C. subternata* plants require more severe drought stress conditions to alter these characteristics. As a result, additional drought stress research addressing these issues is required. Proteomics analysis, however, revealed that *C. subternata* responded to drought stress by altering the expression pattern of a variety of proteins involved in several processes. These findings will help to improve honeybush breeding programmes for the development of drought-tolerant plants. Future studies are required to better understand the stress responsive mechanism in *C. subternata* when subjected to prolonged drought stress under field conditions. Furthermore, the drought response of other *Cyclopia* species, particularly resprouters, also needs investigation in future. In addition to the short duration of the stress treatment, another limitation of the present study is that it did not take genetic variation between the plants into account.

Declaration of Competing Interest

The authors declare that they have no known competing financial interests or personal relationships that could have appeared to influence the work reported in this paper.

Acknowledgements

The authors would like to acknowledge funding by the Department of Science & Innovation (DSI) (DST/CON 0023/2015 to CB), and National Research Foundation (Grant 107805 to EJ), ARC Professional Development Program (PhD bursary to GSM). Gadija Mohamed of the Proteomics Laboratory of the University of Western Cape, Proteomic Laboratory assisted with proteomics, while Nico Walters and George Dico of the Plant Bioactives Group assisted with HPLC analysis of samples and processing of plant material, respectively. The results of the present study are from a PhD dissertation by GSM, accepted in 2020. Two papers on a follow-up study were recently published by CB and co-workers (Water SA 2023, 49(1), 64–72. 10.17159/wsa/2023.v49.i1.3988; Plants 2023, 12, 2181. 10.3390/plants12112181) while the present paper was under review.

Supplementary materials

Supplementary material associated with this article can be found, in the online version, at doi:10.1016/j.sajb.2023.07.042.

References

- Abraham, E., Hourton-Cabassa, C., Erdei, L., Szabados, L., 2010. Methods for determination of proline in plants. Chapter 20. In: Sunker, R. (Ed.), *Plant Stress tolerance. Methods in Molecular Biology*, p. 639. https://doi.org/10.1007/978-1-160761-702-0_20.
- Ahmed, S., Griffin, T.S., Kraner, D., Schaffner, M.K., Sharma, D., Hazel, M., Leitch, A.R., Orians, C.M., Han, W., Stepp, J.R., Robbat, A., Matyas, C., Long, C., Xue, D., Houser, R.F., Cash, S.B., 2019. Environmental factors variably impact tea secondary metabolites in the context of climate change. *Front. Plant Sci.* 10, 939. <https://doi.org/10.3389/fpls.2019.00939>.
- Ain-Lhout, F., Zunzunegui, M., Barradas, D., Tirado, R., Clavijo, A., Garcia Novo, F., 2001. Comparison of proline accumulation in two Mediterranean shrubs subjected to natural and experimental water deficit. *Plant Soil* 230, 175–183. <https://doi.org/10.1023/a:1010387610098>.
- Ali, A.E.E., Husselmann, L.H., Tabb, D.L., Ludidi, N., 2023. Comparative proteomics analysis between maize and sorghum uncovers important proteins and metabolic pathways mediating drought tolerance. *Life* 13 (1), 170. <https://doi.org/10.3390/life13010170>.
- Alvarez, M.E., Savouré, A., Szabados, L., 2022. Proline metabolism and regulatory hub. *Trends Plant Sci.* 27, 39–55. <https://doi.org/10.1016/j.tplants.2021.07.009>.
- Amnan, A.M.N., Aizat, W., Khaidzar, F.D., Tan, B.C., 2022. Drought stress induces morpho-physiological and proteome changes of *Pandanus amaryllifolius*. *Plants* 11, 221. <https://doi.org/10.3390/plants11020221>.
- An, J., Kim, S.H., Bahk, S., Vuong, U.T., Nguyen, N.H., Do, H.L., Kim, S.H., Chung, W.S., 2021. Naringenin induces pathogen resistance against *Pseudomonas syringae* through the activation of NPR1 in Arabidopsis. *Front. Plant Sci.* 12, 672552. <https://doi.org/10.3389/fpls.2021.672552>.
- Armeni, T., Cianfruglia, L., Piva, F., Urbanelli, L., Caniglia, M.L., Pugnali, A., Principato, G., 2014. S-D-Lactoylglutathione can be an alternative supply of mitochondrial glutathione. *Free Radical Biol. Med.* 67, 451–459. <https://doi.org/10.1016/j.freeradbiomed.2013.12.005>.
- Barnes, R.J., Dhanoa, M.S., Lister, S.J., 1989. Standard Normal Variate transformation and de-trending of near-infrared diffuse reflectance spectra. *Appl. Spectrosc.* 43, 772–777. <https://doi.org/10.1366/0003702894022201>.
- Bashir, N., Athar, H.R., Kalaji, H.M., Wróbel, J., Mahmood, S., Zafar, Z.U., Ashraf, M., 2021. Is photoprotection PSII one of the key mechanisms for drought tolerance in maize. *Int. J. Mol. Sci.* 22, 13490. <https://doi.org/10.3390/ijms222413490>.
- Bern, M., Kil, Y.J., 2011. Comments on unbiased statistical analysis for multi-stage proteomic search strategies. *J. Proteome Res.* 10, 2123–2127. <https://doi.org/10.1021/pr101143m>.
- Bijalwan, P., Sharma, M., Kausik, P., 2022. Review of the effects of drought stress on plants, a systematic approach. Preprints. <https://doi.org/10.20944/preprints202202.0014.v1>.
- Blum, A., 2011. *Plant Breeding For Water-Limited Environments*. Springer Verlag, New York, USA.
- Bradford, M.M.A., 1976. Rapid and sensitive method for the quantitation of microgram quantities of protein utilizing the principle of protein-dye binding. *Ann. Biochem.* 7, 248–254. <https://doi.org/10.1016/abio.1976.9999>.
- Brossa, R., Pinto-Marijuan, M., Fransisco, R., Lopez-Carbonell, M., Chaves, M.M., Alegre, L., 2015. Redox proteomics and physiological responses in *Cistus albidus* shrubs subjected to long-term summer drought followed by recovery. *Planta* 241, 803–822. <https://doi.org/10.1007/s00425-014-2221-0>.
- Brestic, M., Allakhverdiev, S.I., 2007. Photosynthesis under biotic and abiotic environmental stress. *Cells* 11, 3953. <https://doi.org/10.3390/cells11243953>.
- Brink, C., Postma, A., Jacobs, K., 2017. Rhizobial diversity and function in rooibos (*Aspalathus linearis*) and honeybush (*Cyclopia* spp.) plants, a review. *S. Afr. J. Bot.* 110, 80–86. <https://doi.org/10.1016/j.sajb.2016.10.025>.
- Cai, B., Ning, Y., Li, Q., Li, Q., Ai, X., 2022. Effects of chloroplast fructose-1,6-bisphosphate aldolase gene on growth and low-temperature tolerance of tomato. *Int. J. Mol. Sci.* 23, 728. <https://doi.org/10.3390/ijms23020728>.
- Carrera, D.A., George, G.M., Fischer-Stettler, M., Galbier, F., Eicke, S., Truenet, E., Streb, S., Zeeman, S., 2021. Distinct plastid fructose bisphosphate aldolases function in photosynthetic and non-photosynthetic metabolism in *Arabidopsis*. *J. Exp. Bot.* 72 (10), 3739–3755. <https://doi.org/10.1093/jxb/erab099>.
- Chakraborty, S., Gogoi, M., Chakravorty, D., 2015. Lactoylglutathione lyase, a critical enzyme in methylglyoxal detoxification, contributes to the survival of *Salmonella* in the nutrient-rich environment. *Virulence* 6, 50–65. <https://doi.org/10.4161/21505594.2014.983791>.
- Chang, L., Wang, L., Peng, C., Tonga, Z., Wang, D., Ding, G., Xiao, J., Guo, A., Wang, X., 2019. The chloroplast proteome response to drought stress in cassava leaves. *Plant Physiol. Biochem.* 142, 351–362. <https://doi.org/10.1016/j.plaphy.2019.07.025>.
- Chen, K.M., Gong, H.J., Chen, G.C., Wang, S.M., Zhang, C.L., 2004. Gradual drought under field conditions influences the glutathione metabolism, redox balance and energy supply in spring wheat. *J. Plant Growth Regul.* 23, 20–28. <https://doi.org/10.1007/s00344-003-0053-4>.
- Chen, T., Riaz, S., Davey, P., Zhao, Z., Sun, Y., Dyke, G.F., Zhou, F., Hartwell, J., Lawson, T., Nixon, P.J., Lin, Y., Liu, L.N., 2023. Producing fast and active Rubisco in tobacco to enhance photosynthesis. *Plant Cell* 35 (2), 795–807. <https://doi.org/10.1093/plcell/koac348>.
- De Beer, D., Schulze, A.E., Joubert, E., De Villiers, A., Malherbe, C.J., Stander, M.A., 2012. Food ingredient extracts of *Cyclopia subternata* (honeybush), variation in phenolic composition and antioxidant capacity. *Molecules* 17, 14602–14624. <https://doi.org/10.3390/molecules171214602>.
- Decker, D., Kleczkowski, L.A., 2019. UDP-sugar producing pyrophosphorylases: distinct and essential enzymes with overlapping substrate specificities, providing de novo precursors for glycosylation reactions. *Front. Plant Sci.* 9, 1822. <https://doi.org/10.3389/fpls.2018.01822>.
- Diniz, A.L., da Silva, D.I.R., Lembke, C.G., Costa, M.D.B.L., Ten-Caten, F., Li, F., Vilela, R.D., Menossi, M., Ware, D., Endres, L., Souza, G.M., 2020. Amino acid and carbohydrate metabolism are coordinated to maintain energetic balance during drought in sugarcane. *Int. J. Mol. Sci.* 21, 9124. <https://doi.org/10.3390/ijms21239124>.
- Dubois, M., Gilles, K.A., Hamilton, J.K., Rebers, P.A., Smith, F., 1956. Colorimetric method for determination of sugars and related substances. *Anal. Chem.* 28, 350–356. <https://doi.org/10.1021/ac60111a017>.
- Dumschott, K., Dechognat, J., Merchant, A., 2019. Water deficit elicits a transcriptional response of genes governing p-nitro biosynthesis in soybean (*Glycine max*). *Int. J. Mol. Sci.* 20, 2411. <https://doi.org/10.3390/ijms20102411>.
- Gharibi, S., Tabatabaei, B.E.S., Saedi, G., Goli, S.A.H., 2016. Effect of drought stress on total phenolic, lipid peroxidation, and antioxidant activity of *Achillea* species. *Appl. Biochem. Biotechnol.* 178, 796–809. <https://doi.org/10.1007/s12010-015-1909-3>.
- Goharrizi, K.J., Hamblin, M.R., Karami, S., Nazari, M., 2021. Physiological, biochemical, and metabolic responses of abiotic plant stress: salinity and drought. *Turk. J. Bot.* 45, 623–642. <https://doi.org/10.3906/bot-2108-30>.
- González, E.M., 2023. Drought stress tolerance in plants. *Int. J. Mol. Sci.* 24 (7), 6562. <https://doi.org/10.3390/ijms24076562>.
- Grosling, M., 2019. Study finds that climate change threatens fynbos. Online. Available from <https://www.news24.com/Green/News/study-finds-that-climate-threatens-fynbos-20170519> (Accessed May, 11).
- Hasanuzzaman, M., Nahar, K., Anee, T.J., Khan, M.I.R., Fujita, M., 2018. Silicon-mediated regulation of antioxidant defense and glyoxalase systems confers drought stress tolerance in *Brassica napus* L. *S. Afr. J. Bot.* 115, 50–57. <https://doi.org/10.1016/j.sajb.2017.12.006>.
- Hou, Q., Li, S., Shang, C., Wen, Z., Cai, X., Hong, Y., Qiao, G., 2022. Genome-wide characterisation of chalcone synthase genes in sweet cherry and functional characterisation of CpCHS1 under drought stress. *Front. Plant Sci.* 13, 989959. <https://doi.org/10.3389/fpls.2022.989959>.
- Hura, T., Hura, K., Ostrowska, A., 2022. Drought-stress induced physiological and molecular changes in plants. *Int. J. Mol. Sci.* 23, 4698. <https://doi.org/10.3390/ijms23094698>.
- Jansen, J.J., Hoefsloot, H.C.J., Van Der Greef, J., Timmerman, M.E., Westerhuis, J.A., Smilde, A.K., 2005. ASCA, analysis of multivariate data obtained from an experimental design. *J. Chemom.* 19, 469–481. <https://doi.org/10.1002/cem.952>.
- Kabbadj, A., Makoudi, B., Mouradj, M., Pauly, N., Frendo, P., Ghoulam, C., 2017. Physiological and biochemical responses involved in water deficit tolerance of nitrogen-fixing *Vicia faba*. *PLoS One* 12, e0190284. <https://doi.org/10.1371/journal.pone.0190284>.
- Kausar, R., Wang, X., Komatsu, S., 2022. Crop proteomics abiotic stress, from data to insights. *Plants* 11, 2877. <https://doi.org/10.3390/plants11212877>.
- Khoza, T.G., Dubery, I.A., Piater, L.A., 2019. Identification of candidate ergosterol-responsive proteins associated with the plasma membrane of *Arabidopsis thaliana*. *Int. J. Mol. Sci.* 20, 1302. <https://doi.org/10.3390/ijms20061302>.
- Khodadadi, E., Fakheri, B.A., Aharizad, S., Emamjomeh, A., Norouzi, M., Komatsu, S., 2017. Leaf proteomics of drought-sensitive and tolerant genotypes of fennel. *BBA-Protein Proteomics* 1865, 1433–1444. <https://doi.org/10.1016/j.bbapap.2017.08.012>.
- Kidwai, M., Ahmad, I.Z., Chakrabarty, D., 2020. Class III peroxidase, an indispensable enzyme for biotic/abiotic stress tolerance and a potent candidate for crop improvement. *Plant Cell Rep.* 39, 1381–1393. <https://doi.org/10.1007/s00299-020-02588-y>.
- Kornienko, N., Zhang, J.Z., Sakimoto, K.K., Yang, P., Reisner, E., 2018. Interfacing nature's catalytic machinery with synthetic materials for semi-artificial photosynthesis. *Nat. Nanotechnol.* 13, 890–899. <https://doi.org/10.1038/s41565-018-0251-7>.
- Kritzinger, H., 2014. *Seasonal Patterns in Carbohydrates and Macronutrients in Southern Highbush Blueberry Plants*. MSc (Horticulture) thesis. Stellenbosch University, Stellenbosch.
- Kumar, S., Trivedi, P., 2018. Glutathione S-transferases, role in combating abiotic stresses including arsenic detoxification in plants. *Front. Plant Sci.* 9, 751. <https://doi.org/10.3389/fpls.2018.00751>.
- Li, H., Li, Y., Ke, Q., Kwak, S.S., Zhang, S., Deng, X., 2020. Physiological and differential proteomic analyses of imitation drought stress response in *Sorghum bicolor* root at the seedling stage. *Int. J. Mol. Sci.* 21 (23), 9174. <https://doi.org/10.3390/ijms21239174>.
- Lin, X., Sun, D.-W., 2020. Recent developments in vibrational spectroscopic techniques for tea quality and safety analyses. *Trends Food Sci. Technol.* 104, 163–176. <https://doi.org/10.1016/j.tifs.2020.06.009>.
- Liou, G., Chiang, Y.C., Wang, Y., Weng, J.K., 2018. Mechanistic basis for the evolution of chalcone synthase catalytic cysteine reactivity in land plants. *J. Biol. Chem.* 293, 18601–18612. <https://doi.org/10.1074/jbc.RA118.005695>.
- Lotter, D., Valentine, A.J., Van Garderen, E.A., Tadross, M., 2014. Physiological responses of a fynbos legume, *Aspalathus linearis* to drought stress. *S. Afr. J. Bot.* 94, 218–223. <https://doi.org/10.1016/j.sajb.2014.07.005>.
- Luz, L.M., Alves, E.C., Vilhena, N.Q., Oliveira, T.B., Silva, Z.G.B., Freitas, J.M.N., Neto, C.F.O., Costa, R.C.L., Costa, L.C., 2023. Distinct physiological mechanism underpin growth

- and rehydration of *Hymenaea courbaril* and *Hymenaea stigonocarpa* upon short-term exposure to drought stress. *J. For. Res.* 34, 113–123. <https://doi.org/10.1007/s11676-022-01558-2>.
- Mabizela, G.S., Muller, M., De Beer, D., Van der Rijst, M., Slabbert, M.M., Joubert, E., Bester, C., 2020. Effect of genotype and harvest season on quality characteristics of *Cyclopia subternata*, phenolic content and sensory profile. *S. Afr. J. Bot.* 132, 491–501. <https://doi.org/10.1016/j.sajb.2020.06.010>.
- Mahmoud, O.M.B., Hidri, R., Talbi-Zribi, O., Taamali, W., Abdelly, C., Djebali, N., 2020. Auxin and proline producing rhizobacteria mitigate salt-induced growth inhibition of barley plants by enhancing water and nutrient status. *S. Afr. J. Bot.* 128, 209–217. <https://doi.org/10.1016/j.sajb.2019.10.023>.
- Manley, M., 2014. Near-infrared spectroscopy and hyperspectral imaging: non-destructive analysis of biological materials. *Chem. Soc. Rev.* 43, 8200–8214. <https://doi.org/10.1039/C4CS00062E>.
- Mao, Y., Li, H., Wang, Y., Fan, K., Song, Y., Han, X., Zhang, J., Ding, S., Song, D., Wang, H., Ding, Z., 2022. Prediction of tea polyphenols, free amino acids and caffeine content in tea leaves during wilting and fermentation using hyperspectral imaging. *Foods* 11, 2537. <https://doi.org/10.3390/foods11162537>.
- Masike, K., de Villiers, A., de Beer, D., Joubert, E., Stander, M.A., 2022. Application of direct injection-ion mobility spectrometry-mass spectrometry (DI-IMS-MS) for the analysis of phenolics in honeybush and rooibos tea samples. *J. Food Compos. Anal.* 106, 104308. <https://doi.org/10.1016/j.jfca.2021.104308>.
- Mattioli, R., Palombi, N., Funck, D., Trovalto, M., 2020. Proline accumulation in pollen grains as potential target for improved yield stability under salt stress. *Front. Plant Sci.* 11, 582877. <https://doi.org/10.3389/fpls.2020.582877>.
- Mehari, T.G., Xu, G., Magangwa, R.O., Umer, M.J., Kirungu, J.N., Cai, X., Hou, Y., Wang, Y., Yu, S., Wang, K., Zhou, Z., Liu, F., 2021. Genome wide identification and characterization of light-harvesting chloro a/b binding (LHC) genes reveals their potential role in enhancing drought tolerance in *Gossypium hirsutum*. *J. Cotton Res.* 4, 5. <https://doi.org/10.1186/s42397-021-00090-8>.
- Muneer, S., Kim, T.H., Choi, B.C., Lee, B.S., Lee, J.H., 2014. Effect of CO, NO_x and SO₂ on ROS production, photosynthesis and ascorbate-glutathione pathway to induce *Fragaria × annasa* as hyperaccumulator. *Redox. Biol.* 2, 91–98. <https://doi.org/10.1016/j.redox.2013.12.006>.
- Nahar, K., Hsanuzzaman, M., Alam, M.M., Rahman, A., Mahmud, J.A., Suzuki, T., Fujita, M., 2017. Insights into spermine-induced combined high temperature and drought tolerance in mung bean, osmoregulation and roles of antioxidant and glyoxalase system. *Protoplasma* 254, 445–460. <https://doi.org/10.1007/s00709-016-0965-z>.
- Naik, B., Kumar, V., Rizwanuddin, S., Chauhan, M., Choudhary, M., Gupta, A.K., Kumar, P., Kumar, V., Saris, P.K.J., Rather, M.A., Bhuyan, S., Neog, P.R., Mishra, S., Rustagi, S., 2023. Genomics, proteomics and metabolomics approaches to improve abiotic stress in tomato plant. *Int. J. Mol. Sci.* 24, 3025. <https://doi.org/10.3390/ijms24033025>.
- Nan, N., Wang, J., Shi, Y., Qian, Y., Jiang, Y., Huang, S., Liu, Y., Wu, Y., Liu, B., Xu, Z.Y., 2020. Rice plastidial NAD-dependent malate dehydrogenase 1 negatively regulates salt stress response by reducing the vitamin B6 content. *Plant Biotechnol. J.* 18 (1), 172–184. <https://doi.org/10.1111/pbi.13184>.
- Næs, T., Brockhoff, P., Tomic, O., 2010. *Statistics For Sensory and Consumer Science*. Wiley, New York, USA. <https://doi.org/10.1002/9780470669181>.
- Nazari, M., Moosavi, S.S., Maleki, M., Goharizi, K.J., 2020. Chloroplastic acyl carrier protein synthase I and chloroplastic 20 kDa chaperonin proteins are involved in wheat (*Triticum aestivum*) in response to moisture stress. *J. Plant Interact.* 15 (1), 180–187. <https://doi.org/10.1080/17429145.2020.1758812>.
- Ostrowski, M., Ciarkowska, A., Dlka, A., Wilmowicz, E., Jakubowska, A., 2020. Biosynthesis pathway of indole-3-acetyl-myo-inositol during development of maize (*Zea mays* L.) seeds. *J. Plant Physiol.* 245, 153082. <https://doi.org/10.1016/j.jplph.2019.153082>.
- Ott, L., 1998. *An Introduction to Statistical Methods and Data Analysis*, 3rd ed. PWS-Kent Publishing Company, Boston.
- Panara, F., Passeri, V., Lopez, L., Porceddu, A., Calderini, O., Paolucci, F., 2022. Functional characterization of MtrGSTF7, a glutathione S-transferase essential for anthocyanin accumulation in *Medicago truncatula*. *Plants* 11 (10), 1318. <https://doi.org/10.3390/plants11101318>.
- Perin, E.C., Messias, R.S., Galli, V., Borowski, M., De Souza, E.R., De Avila, L.O., Bamberg, A.L., Rombaldi, C.V., 2019. Mineral content and antioxidant compounds in strawberry fruit submitted to drought stress. *Food Sci. Technol.* 39, 245–254. doi: <https://doi.org/10.1590/fst.09717>.
- Pirovich, D.B., Da'dara, A.A., Skelly, P.J., 2021. Multifunctional fructose 1,6-biphosphate aldolase as a therapeutic target. *Front. Mol. Biosci.* 8, 719678. <https://doi.org/10.3389/fmolb.2021.719678>.
- Podda, A., Pollastri, S., Bartolini, P., Pisutto, C., Pellegrini, E., Nali, C., Cencetti, G., Michelozzi, M., Frassinetti, S., Giorgetti, L., Fineschi, S., Del Carratole, R., Masert, B., 2019. Drought stress modulates secondary metabolites in *Brassica oleracea* L. var. *acephala* (DC) Alef, var. *sabellica* L. *J. Sci. Food Agric.* 99, 5533–5540. <https://doi.org/10.1002/jsfa.9816>.
- Postma, A., Slabbert, E., Postma, F., Jacobs, K., 2016. Soil bacterial communities associated with natural and commercial *Cyclopia* spp. *FEMS Microbiol. Ecol.* 92. <https://doi.org/10.1093/femsec/fiw016>.
- Qian, W., Hu, J., Zhang, X., Zhao, L., Wang, Y., Ding, Z., 2018. Response of tea plants to drought stress. In: Han, W.-Y., Li, X., Ahammed, G.J. (Eds.), *Stress Physiology of Tea in the Face of Climate Change*. Springer, Singapore, Singapore, pp. 63–81. https://doi.org/10.1007/978-981-13-2140-5_4.
- Qin, C.X., Chen, Z.L., Wang, M., Li, A.M., Liao, F., Li, Y., Wang, M.Q., Long, M.H., Lakshmanan, P., Huang, D.L., 2021. Identification of proteins and metabolic networks associated with sucrose accumulation in sugarcane (*Saccharum* spp. interspecific hybrids). *J. Plant Interact.* 16, 166–178. <https://doi.org/10.1080/17429145.2021.1912840>.
- Rabatel, G., Marini, F., Walczak, B., Roger, J.M., 2019. VSN, variable sorting for normalization. *J. Chemom.* 34, e3164. <https://doi.org/10.1002/cem.3164>.
- Rasool, F., Uzair, M., Naeem, M.K., Rehman, N., Afroz, A., Shah, H., Khan, M.R., 2021. Phenylalanine ammonia-lyase (PAL) genes family in wheat (*Triticum aestivum* L.) genome wide characterization and expression profiling. *Agronomy* 11, 2511. <https://doi.org/10.3390/agronomy11122511>.
- Rodriguez-Calzada, T., Qian, M., Strid, A., Neugart, S., Schreiner, M., Torres-Pacheco, I., Guevara-Gonzales, R.G., 2019. Effect of UV-B radiation on morphology, phenolic compound production, gene expression, and subsequent drought stress responses in chili pepper (*Capsicum annuum* L.). *Plant Physiol. Biochem.* 134, 94–102. <https://doi.org/10.1016/j.plaphy.2018.06.025>.
- Sade, N., Galkin, E., Moshelion, M., 2015. Measuring *Arabidopsis* tomato and barley leaf relative water content (RWC). *Bio Protoc.* 5, e1451. <https://doi.org/10.21769/Bio-Protoc.1451>.
- Sasi, S., Venkatesh, J., Daneshi, R.F., Gururani, M.A., 2018. Photosystem II extrinsic proteins and their putative. *Plants* 7, 100. <https://doi.org/10.3390/plants7040100>.
- Shanker, A.K., Amirineni, S., Bhanu, D., Yadav, S.K., Jyothilakshmi, N., Vanaja, M., Singh, J., Sarkar, B., Maheswari, M., Singh, V.K., 2022. High resolution dissection of photosystem II electron transport reveals differential response to water deficit and heat stress in isolation and combination in pearl millet (*Pennisetum glaucum* (L.) R. Br.). *Front. Plant Sci.* 13, 892676. <https://doi.org/10.3389/fpls.2022.892676>.
- Shapiro, S.S., Wilk, M.B., 1965. An analysis of variance test for normality (complete samples). *Biometrika* 52, 591. <https://doi.org/10.2307/2333709>.
- Shayan, S., Norouzi, M., Vahed, M.M., Mohammadi, S.A., Toorchi, M., 2020. Leaf proteome pattern of two bread wheat varieties under water deficit stress conditions. *Curr. Plant Biol.* 23, 100146. <https://doi.org/10.1016/j.cpb.2020.100146>.
- Sherin, G., Aswathi, K.P.R., Puthur, J.T., 2022. Photosynthetic functions in plants subjected to stresses are positively influenced by priming. *Plant Stress* 4, 100079. <https://doi.org/10.1016/j.stress.2022.100079>.
- Shigetou, J., Tsutsumi, Y., 2016. Diverse functions and reactions of class III peroxidases. *New Phytol.* 209 (4), 1395–1402. <https://doi.org/10.1111/nph.13738>.
- Singh, M., Kumar, V., Kumar, L., 2020. Functional analysis of chalcone synthase (CSH) gene in Indian wheat cultivars in response to PEG-induced drought stress. *Int. J. Curr. Microbiol. Appl. Sci.* 9, 833–840. <https://doi.org/10.20546/ijcmas.2020.910.099>.
- Singh, P.K., Indoliya, Y., Agrawal, L., Awasthi, S., Deeba, F., Dwivedi, S., Chakrabarty, D., Shirke, P.A., Pandey, V., Singh, N., Dankher, O.P., Barik, S.K., Tripathi, R.D., 2022. Genomic and proteomic responses to drought stress and biotechnological interventions of enhanced drought tolerance in plants. *Curr. Biol.* 29, 100239. <https://doi.org/10.1016/j.cpb.2022.100239>.
- Slabbert, E.L., Malgas, R.R., Veldtman, R., Addison, P., 2011. Honeybush (*Cyclopia* spp.) phenology and associated arthropod diversity in the Overberg region, South Africa. *Bothalia* 49 (1), a2430. <https://doi.org/10.4102/abc.v49i1.2430>.
- Slabbert, M.M., Kruger, G., 2014. Antioxidant enzyme activity, proline accumulation, leaf area and cell membrane stability in water-stressed *Amaranthus* leaves. *S. Afr. J. Bot.* 95, 123–128. <https://doi.org/10.1016/j.sajb.2014.08.008>.
- Spormann, S., Nadais, P., Sousa, F., Pinto, M., Martins, M., Sousa, B., Fidalgo, F., Soares, C., 2023. Accumulation of proline in plants under contaminated soils, are we on the same page. *Antioxidants* 12 (3), 666. <https://doi.org/10.3390/antiox12030666>.
- Tonhati, R., Mello, S.C., Momessoc, P., Pedroso, R.M., 2020. L-Proline alleviates heat stress of tomato plants grown under protected environment. *Sci. Hortic.* 268, 109370. <https://doi.org/10.1016/j.scienta.2020.109370>.
- Tolrà, R., Martos, S., Hajiboland, R., Poschenrieder, C., 2020. Aluminium alters mineral composition and polyphenol metabolism in leaves of tea plants (*Camellia sinensis*). *J. Inorg. Biochem.* 204, 110–956. <https://doi.org/10.1016/j.jinorgbio.2019.110956>.
- Vayghan, H.S., Nawrocki, W.J., Schiphorst, C., Tollerer, D., Hu, C., Douet, V., Glauser, G., Finazzi, G., Croce, R., Wientjes, E., Longoni, F., 2022. Photosynthetic light harvesting and thylakoid organization in a CRISPR/Cas9 *Arabidopsis thaliana* LHCB1 knockout mutant. *Front. Plant Sci.* 13, 833032. <https://doi.org/10.3389/fpls.2022.833032>.
- Wang, L., Jin, X., Li, Q., Wang, X., Li, Z., Wu, X., 2016. Comparative proteomics reveals that phosphorylation of β carbonic anhydrase 1 might be important for adaptation to drought stress in *Brassica napus*. *Sci. Rep.* 6, 39024. <https://doi.org/10.1038/srep39024>.
- Wang, X., Liu, H., Zhang, D., Zou, D., Wang, J., Zheng, H., Jia, Y., Qu, Z., Sun, B., Zhao, H., 2022. Photosynthetic carbon fixation and sucrose metabolism supplemented by weighted gene co-expression network analysis in response to water stress in rice with overlapping growth stages. *Front. Plant Sci.* 13, 864605. <https://doi.org/10.3389/fpls.2022.864605>.
- Wang, Y., Liao, J., Wu, J., Huang, H., Yuan, Z., Yang, W., Wu, X., Li, X., 2022. Genome-wide identification and characterization of soybean DEAD-Box gene family and expression response to rhizobia. *Int. J. Mol. Sci.* 23, 1120. <https://doi.org/10.3390/ijms23031120>.
- Wassie, W.A., Anduale, A.M., Molla, A.E., Tarekeng, Z.G., Aragaw, M.W., Ayana, M.T., 2023. Growth, physiological, and biochemical responses of Ethiopian red pepper (*Capsicum annuum* L.) cultivars to drought stress. *Sci. World J.* 4374318. <https://doi.org/10.1155/2023/4374318>.
- Wold, S., Geladi, P., Esbensen, K., Ohman, J., 1987. Multi-way principal components-and PLS-analysis. *J. Chemom.* 1, 41–56. <https://doi.org/10.1002/cem.1180010107>.
- Wu, J., Wang, J., Hui, W., Zhao, F., Wang, P., Su, C., Wei, G., 2022. Physiology of plant responses to water stress and related gene a review. *Forests* 13, 324. <https://doi.org/10.3390/f13020324>.
- Xia, J., Xin, W., Wang, F., Xei, W., Liu, Y., Xu, J., 2022. Cloning and characterization of fructose-1,6-biphosphate aldolase from *Euphorbia superba*. *Int. J. Mol. Sci.* 23 (18), 10478. <https://doi.org/10.3390/ijms231810478>.

- Xu, C., Xu, Y., Ang, B., 2008. Protein extraction for two-dimensional gel electrophoresis of proteomic profiling in turfgrass. *Crop Sci.* 48, 1608–1614. <https://doi.org/10.2135/cropsci2007.11.0624>.
- Xu, L., Hu, Y., Jin, G., Lei, P., Sang, L., Luo, Q., Liu, Z., Guan, F., Meng, F., Zhao, X., 2021. Physiological and proteomic responses to drought in leaves of *Amygdalus mira* (Koenne) Yü et Lu. *Front. Plant Sci.* 12, 620499. <https://doi.org/10.3389/fpls.2021.620499>.
- Yang, Y.J., Shi, Q., Sun, H., Mei, R.Q., Huang, W., 2022. Differential response of photosynthetic machinery to fluctuating light in mature and young leaves of *Dendrobium officinale*. *Front. Plant Sci.* 12, 829783. <https://doi.org/10.3389/fpls.2021.829783>.
- Ye, T., Shi, H., Wang, Y., Chan, Z., 2015. Contrasting changes caused by drought and submergence stresses in bermudagrass (*Cynodon dactylon*). *Front. Plant Sci.* 6, 951. <https://doi.org/10.3389/fpls.2015.00951>.
- Yilmaz, P., Babat, C.F., Yilmaz, C., 2023. Comparison of short-term physiological and biochemical effects of drought stress on two wheat cultivars. *Agric. Agribus. Biotechnol.* 66, e23220705. <https://doi.org/10.1590/1678-4324-2023220705>.
- Yin, H., Yang, F., He, X., Du, X., Mu, P., Ma, W., 2022. Advances in functional study of glutamine synthase in plant biotic stress tolerance response. *Crop J.* 10, 917–923. <https://doi.org/10.1016/j.cj.2022.01.003>.
- Yoshida, T., Malherbe, C.J., Okon, K., Miura, Y., Hattori, M., Matsuda, H., Muller, C.J.F., Joubert, E., 2020. Enhanced production of Th1- and Th2-type antibodies and induction of regulatory T cells in mice by oral administration of *Cyclopia* extracts with similar phenolic composition to honeybush herbal tea. *J. Funct. Foods* 64, 103704. <https://doi.org/10.1016/j.jff.2019.103704>.
- Zhang, Y., He, J., Xiao, Y., Zhang, Y., Liu, Y., Wan, S., Liu, L., Dong, Y., Liu, H., Yu, Y., 2021. CsGSTU8, a glutathion s-transferase from *Camelia sinensis* is regulated by CsWRKY48 and plays a positive role in drought tolerance. *Front. Plant Sci.* 12, 795919. <https://doi.org/10.3389/fpls.2021.795919>.
- Zhao, Y., Yu, H., Zhou, J.M., Smith, S.M., Li, J., 2020. Malate circulation, linking chloroplast metabolism to mitochondrial ROS. *Trends Plant Sci.* 25, 446–454. <https://doi.org/10.1016/j.tplants.2020.01.010>.
- Zhou, P., Graether, S.P., HU, L., Zhang, W., 2023. The role of proteins in plants under abiotic stress. *Front. Plant Sci.* 14, 1193542. <https://doi.org/10.3389/fpls.2023.1193542>.
- Zhunge, X.L., Xu, H., Xiu, Z.J., Yang, H.L., 2020. Biochemical functions of glutathione S-transferase family of *Salix babylonica*. *Front. Plant Sci.* 11, 364. <https://doi.org/10.3389/fpls.2020.00364>.